A techno-economic assessment of the viability of a photovoltaic-wind-battery storage-hydrogen energy system for electrifying primary healthcare centre in Sub-Saharan Africa.

Energy Conversion and Management: X 23 (2024) 100643

Contents lists available at ScienceDirect

Energy Conversion and Management: X

journal homepage: www.sciencedirect.com/journal/energy-conversion-and-management-x

A techno-economic assessment of the viability of a photovoltaic-wind-battery storage-hydrogen energy system for electrifying primary healthcare centre in Sub-Saharan Africa

Oluwaseye Samson Adedoja [a,b,*], Emmanuel Rotimi Sadiku [a,b], Yskandar Hamam [c,d]

[a] Department of Chemical, Metallurgical and Materials Engineering, Tshwane University of Technology, Pretoria, South Africa
[b] Institute of Nano Engineering Research (INER), Tshwane University of Technology, Pretoria, South Africa
[c] Department of Electrical Engineering, Tshwane University of Technology, Pretoria, South Africa
[d] Ecole Superieure d'Ingenieurs en Electrotechnique et Electronique, 2 Boulevard Blaise Pascal, 93160 Noisy-Le-Grand, France

ARTICLE INFO

Keywords:
Solar PV
Primary Healthcare
Hydrogen energy
Techno-economic assessment
Sub-Saharan Africa

ABSTRACT

Healthcare facilities in isolated rural areas of sub-Saharan Africa face challenges in providing essential health services due to unreliable energy access. This study examines the use of hybrid renewable energy systems consisting of solar PV, wind turbines, batteries, and hydrogen storage for the electrification of rural healthcare facilities in Nigeria and South Africa. The study deployed the efficacy of Hybrid Optimization of Multiple Energy Resources software for techno-economic analysis and the Evaluation based on the Distance from Average Solution method for multi-criteria decision-making for sizing, optimizing, and selecting the optimal energy system. Results show that the optimal configurations achieve cost-effective levelized energy costs ranging from $0.336 to $0.410/kWh for both countries. For the Nigeria case study, the optimal energy system includes 5 kW PV, 10 kW fuel cell, 10 kW inverter, 10 kW electrolyzer, and 16 kg hydrogen tank. South Africa's optimal configuration has 5 kW PV, 10 kW battery, 10 kW inverter, and 7.5 kW rectifier. Solar PV provides more than 90 % of energy, with dual axis tracking yielding the highest output: 8,889kWh/yr for Nigeria and 10,470kWh/yr for South Africa. The multi-criteria decision-making analysis reveals that Nigeria's preferred option is the hybrid system without tracking. In contrast, the horizontal axis, weekly adjustment tracking configuration is optimal for South Africa, considering technical, economic, and environmental criteria. The findings highlight the importance of context-specific optimization for hybrid renewable energy systems in rural healthcare facilities to accelerate Sustainable Development Goals 3 and 7.

Introduction

Just like potable water, energy is one of the critical products on which the sustenance of modern civilization depends; virtually all human activities require energy as input. Energy, especially electricity, is a driver of goods and services, offered in the: industrial (manufacturing), banking, academic, agricultural, and health sectors; it is, therefore, inevitable to modern man [3]. Various initiatives have been implemented globally to improve electricity access. Although there was a 10.5 % decrease in the global population without access to electricity from 2018 to 2019, almost 770 million people worldwide still do not have this crucial service as of 2019 [1]. According to the International Energy Agency, Sub-Saharan Africa has the largest population of individuals lacking access to electricity, surpassing all other continents [26].

The success that resulted in the decline in the number of people without electricity between 2018 and 2019, could be attributed to the momentum gained by adopting decentralized renewable-based solutions. The number of electricity consumers, powered by decentralized grid systems (nano, mini, and micro), has grown from 5 million in 2010 to 11 million in 2019; this is more than 100 percent increment [47]. Despite the various efforts put in place to increase electricity access globally, it is projected that globally, the ripple effects of the COVID-19 pandemic will keep nearly 660 million people (with the majority in sub-Saharan Africa) without electricity by the year 2030 [47]. While since 2013, sub-Saharan Africa has experienced a continuous decline in the number of residents without electricity, this success is set to be reversed, thanks to the COVID-19 pandemic. The COVID-19 pandemic has pulled many countries away from the orbit of attaining universal access to

* Corresponding author.
E-mail address: princeturn205@yahoo.com (O.S. Adedoja).

https://doi.org/10.1016/j.ecmx.2024.100643
Received 29 February 2024; Received in revised form 30 May 2024; Accepted 2 June 2024
Available online 4 June 2024

Nomenclature

Nomenclature/Abbreviation	Description
PV	Photovoltaic
HOMER	Hybrid Optimization of Multiple Energy Resources
EDAS	Evaluation Based on Distance from Average Solution
MCDM	Multi-Criteria Decision-Making
SDGs	Sustainable Development Goals
LCOE	Levelized Cost of Energy
NPC	Net Present Cost
COE	Cost of Energy
TNPC	Total Net Present Cost
LCOH	Levelized Cost of Hydrogen
TA	Two-Axis Tracking
HADA	Horizontal Axis, Daily Adjustment
HAMA	Horizontal Axis, Monthly Adjustment
HAWA	Horizontal Axis, Weekly Adjustment
VACA	Vertical Axis, Continuous Adjustment
HACA	Horizontal Axis, Continuous Adjustment
NT	No Tracking
LF	Load Following
CC	Cycle Charging
CPSO	Constrained Particle Swarm Optimization
GA	Genetic Algorithm
HS	Harmony Search
FPA	Flower Pollination Algorithm
P_{pv}	Power output of the PV array
Y_{pv}	Rated capacity of the PV array
f_{pv}	PV derating factor
$\overline{G_T}$	Solar radiation incident on the PV array
$G_{T,STC}$	Incident radiation at standard test conditions
α_P	Temperature coefficient of power
T_C	PV cell temperature
$T_{C,STC}$	PV cell temperature under standard test conditions
$\eta_{mp,STC}$	Maximum power point efficiency under standard conditions
α	Solar absorptance of the PV array
μ	Solar transmittance of any cover over the PV array
V_h	Wind speed at the hub height
V_m	Wind speed at anemometer height
H_h	Hub height
H_m	Anemometer height
H_m	Power law exponent
ρ	Actual air density
ρ_o	Air density at standard temperature and pressure
$P_{o,STP}$	Wind turbine power output at standard conditions
P_o	Wind turbine power output
$\dot{H}_2$	Hydrogen production rate
η_f	Faraday efficiency
I_e	Electrolyzer current
N_s	Number of electrolyzer cells in series
F	Faraday constant
P_{com}	Electrolyzer compressor power
P_1, P_2	Pressure at the electrolyzer inlet and outlet, respectively
γ	Hydrogen specific heat ratio
T	Temperature
η_{com}	Isentropic efficiency of the compressor
R	Universal gas constant
FC_{ele}	Fuel cell electrical power
LHV_h	Lower heating value of hydrogen
ρ_h	Density of hydrogen
η_{fc}	Fuel cell efficiency
n	Number of batteries
$Batt_{aut}$	Battery autonomy
E_b	Battery energy capacity
V_n	Nominal voltage of a single battery
Q_n	Nominal capacity of a single battery
$C_{h,tank}$	Hydrogen tank capacity
H_{aut}	Hydrogen tank autonomy
E_d	Daily average energy demand
$TNPC$	Total annualized cost
$Q_{lifetime,i}$	lifetime throughput
f_i	number of cycles to failure
d_i	depth of discharge
q_{max}	maximum capacity of the battery

electricity by the year 2030.

Based on the foregoing, it could be seen that as the year 2030 target for the United Nations Sustainable Development Goals (SDG) 7 draws closer, various measures would have to be deployed by the various stakeholders in the energy sector to achieve sustainable and affordable energy for all. One of the measures includes extending the centralized electricity grid (top–bottom approach) to areas with no access but with the required number of customers necessary to break even [10]. In cases where utility companies are not projected to profit, adopting decentralized grid systems is proposed as a bottom-top approach to attaining SDG 7 [10]. Most of these decentralized energy systems are based on renewable energy sources, such as solar PV, wind turbines, and diesel generators for hybridization [6]. Various advantages of adopting renewable energy sources in grid decentralization have been discussed in the literature. The adoption of a renewable energy-based decentralized approach would not only slow down the depletion of conventional energy sources, but it would also reduce the emission of greenhouse gases [45]. It would also aid in the elimination of transmission losses, reduction of poverty, creation of jobs, and most importantly, it could improve the living standards of the host communities [21].

The availability of reliable, clean, and affordable electricity is also a major component of operating clinics and healthcare facilities [8]). For example, for an efficient distribution of temperature-sensitive medications, such as anti-retroviral drugs and vaccines, there is a need for adequate refrigeration, which can only be possible with reliable electricity. Another important aspect of reliable electricity in the health sector is for illumination and operating basic medical equipment, especially for patients requiring emergency care and during child delivery. As reported in the literature [38], the availability of reliable electricity in healthcare facilities can reduce the loss of lives and improve the quality of life; this is one of the significant targets of SDG number 3. With the COVID-19 pandemic that ravaged havoc across the globe, healthcare facilities were overburdened and were expected to cope with the pressures from COVID-19 patients; this is in addition to carrying out routine procedures for other patients.

Various studies have highlighted the profound effects of energy poverty on Sub-Saharan Africa's socioeconomic growth [27]. Lack of access to dependable electricity reduces the prospects for good health care, obstructs economic output, and widens the already-existing disparities between those with access and those without access to electricity [15]. These studies highlight how energy poverty and more so, general development objectives are intertwined. Access to reliable and sustainable energy is essential for improving healthcare, especially in the isolated and underdeveloped areas of Sub-Saharan Africa [39]. The confluence of energy poverty and healthcare concerns in these regions demands creative solutions to closing the gap and improving community wellbeing. Sub-Saharan Africa faces numerous energy-related issues, ranging from unstable power sources to insufficient infrastructure [17].

This study aims to fill the research gap by investigating the feasibility and optimality of hybrid renewable energy systems integrating solar PV, wind turbines, batteries, and hydrogen storage for rural healthcare facilities in sub-Saharan Africa. The novelty of this work lies in the comprehensive techno-economic analysis, the evaluation of different solar tracking configurations, and the application of a multi-criteria decision-making (MCDM) approach using the EDAS method to assess the trade-offs between system parameters and performance.

This study makes three main contributions. First, it presents a detailed framework for designing and optimizing hybrid renewable energy systems for rural healthcare facilities, considering two energy storage technologies and seven solar tracking configurations. Second, it identifies the optimal system configurations for two locations in sub-Saharan Africa, considering site-specific renewable energy resources, healthcare facility energy demands, and economic parameters. Lastly, the study introduces the EDAS method for MCDM that allows for the evaluation of trade-offs between technical, economic, and environmental criteria when selecting the most suitable hybrid system configurations for the two locations.

The results of this study offer valuable insights into developing sustainable energy solutions for healthcare facilities in rural areas of sub-Saharan Africa. This will contribute to the overarching efforts to attain Sustainable Development Goals 3 and 7. The methods and insights can be extended to other regions with comparable challenges, emphasizing the significance of context-specific optimization and decision-making for hybrid renewable energy systems.

Literature review

Several recent studies have focused on the implementation of hybrid renewable energy systems in rural healthcare facilities (Koholé et al., 2024). These studies have examined the technical, economic, and environmental factors involved in combining solar PV, wind turbines, diesel generators, and energy storage technologies to deliver reliable and environmentally friendly electricity to health centers that are not connected to the central power grid. However, the existing literature lacks a comprehensive analysis of the impact of advanced energy storage technologies, such as batteries and hydrogen, and the role of solar tracking configurations in optimizing the performance of hybrid systems.

Yakub et al., explored the use of HRES to improve electricity access in rural Nigerian healthcare institutions affected by the COVID-19 pandemic [48]. The HOMER Pro and RETScreen Expert software were employed to determine the most viable and cost-effective solution energy system. Results show that solar-diesel HRES can save about $30,583 per year, with a net present value of $390,949, a 1.3-year payback period, a 75-ton CO_2 emission reduction, and $30,583 in annual savings over the initial diesel system. An inherent drawback of the study conducted by [48] is the consideration of a single energy storage technology. The inclusion of battery and hydrogen storage technologies could significantly enhance the reliability and dispatchability of the HES, particularly during periods of low renewable energy availability.

In another study, Islam et al., conducted a techno-economic analysis of a hybrid solar-diesel microgrid system for a rural healthcare facility in Bangladesh [29]. The authors used the HOMER software to design a 32 kW rooftop solar PV system with a bi-directional inverter and a 28 kW generator to suit the facility's energy requirements. The economic study revealed that the net present cost was $33,818 at a levelized cost of $0.022/kWh. Compared to the high fuel prices and the pollution from conventional diesel generators alone, the hybrid system was a practical, cost-effective alternative for providing reliable electricity to the rural healthcare center.

Babatunde et al., designed optimal hybrid renewable energy systems for rural healthcare institutions in Nigeria, incorporating solar, wind, diesel generators, and battery storage [14]. PV/diesel/battery was considered the most viable configuration across all geographies, with a net present cost of between $12,779-$13,646, at between 70–80 % renewable portion, and energy costs ranging from $0.507 to $0.542/kWh. A sensitivity study of diesel prices and interest rates investigated the impact of withdrawing fuel subsidies in Nigeria. The hybrid system has been proven to be the best cost-effective alternative for off-grid healthcare institutions in Nigeria. While this study examined battery storage, it did not investigate the potential of hydrogen as an energy storage medium or the impact of solar tracking on energy production. By using the HOMER software, Ighravwe et al., devised a framework to determine the most effective hybrid renewable energy systems (HRES) for ensuring sustainable healthcare services in Nigeria [28]. By employing a multi-criteria decision analysis, incorporating technical, economic, and environmental criteria, the authors determined that the operational and total net present costs were the least and most significant factors, respectively. Six communities' evaluations of the framework indicated that a PV-diesel battery was the optimal HRES option. This research fills the void in knowledge regarding integrating healthcare delivery and energy access objectives to facilitate data-driven HRES planning for off-grid healthcare facilities. Although this study offers a significant foundation for decision-making, it is limited in terms of the depth of technical analysis and the inclusion of hydrogen energy storage technology. The study does not provide detailed simulations or optimization of the hybrid system configurations, limiting the understanding of their performance and feasibility.

Furthermore, Olatomiwa et al. designed optimal hybrid renewable energy systems for rural healthcare centers in Nigeria that lack reliable electricity. By using the HOMER software and long-term meteorological data, they found in Sokoto and Jos, a high wind potential and a strong solar potential, nationwide. The techno-economic analysis determined the fact that the PV/wind/diesel/battery systems were optimal for Iseyin, Sokoto, Maiduguri, Jos, and Enugu, while the PV/diesel/battery was best for Port Harcourt, based on the local renewable resources. Although this research offered significant insights regarding the viability of hybrid systems in rural healthcare facilities, it did not consider the integration of hydrogen storage or the impact of solar tracking on system performance.

Abundant wind and solar make hybrid systems ideal for improving electricity access, healthcare delivery and reducing maternal and child mortalities in the off-grid rural areas of Nigeria. By using the Homer Pro software, Chowdhury et al., developed an ideal hybrid renewable energy system for a temporary COVID-19 healthcare facility in Bangladesh [18]. When compared to diesel-only systems, the PV/converter/wind/battery/diesel generator configuration reduced expenses and emissions. An economic analysis with a seven-year payback period revealed a levelized cost of $0.4688/kWh, and 35 % less than solar household systems. When compared to a diesel-only system, the hybrid system produced 27 % less CO_2, making it environmentally friendly. Healthcare institutions' energy needs are increasing, and optimized hybrid renewable energy systems can assist in fulfilling that demand, while lowering costs and emissions.

Raghuwanshi and Arya used the HOMER software to design and optimize a stand-alone hybrid solar PV system for a rural healthcare facility in India [41]. An economic study revealed that the PV-diesel-battery system had higher starting costs of $2,418, but lower net present costs of $13,523, when compared to $879 and $20,515 for diesel-battery. The hybrid system was more cost-effective and environmentally favorable than standard diesel. The results show that renewable energy systems can be feasible for providing dependable, cost-effective power to off-grid healthcare institutions in remote places. However, the study did not consider the integration of wind energy or hydrogen storage, limiting its applicability to regions with high solar potential. In a similar study, the authors employed the Markov and frequency-duration models to assess the reliability of stand-alone hybrid solar PV systems in remote places [42]. The diesel-only, PV/battery, and PV/diesel/battery setups were evaluated for failure rate, downtime, unavailability, energy not supplied, and loss of load probability. Due to solar resources and the load demand, the hybrid PV/battery/diesel achieved the highest reliability indices. The results showed that hybrid systems are more reliable than diesel-only systems in off-grid scenarios. The framework assists the policymakers in determining the best strategies for energizing rural healthcare facilities. The main emphasis of the study was the evaluation of reliability, with little consideration given to the economic and environmental consequences associated with the various configurations of the systems. Furthermore, the study does not explore the potential of hydrogen storage or the impact of solar tracking on system performance and reliability.

Olatomiwa et al., designed optimized hybrid grid-connected systems that incorporated diesel and renewable energy sources to address the insufficient electricity supply at rural Nigerian healthcare institutions [37]. Simulations using meteorological data and load profiles from six locations showed that solar-wind-diesel systems could meet the demand at low prices of between \$0.0588–0.115/kWh and with good reliability. Most of the generation was produced by wind and solar power. To optimize the operation of hybrid renewable energy systems, linked to an unreliable grid that supplies healthcare facilities in rural Nigeria, Adetoro et al., assessed various dispatch strategies [4]. A comparison was made between the enhanced combined dispatch (ECD) strategy and the load following (LF) and cycle charging (CC) strategies. ECD facilitated the most efficient energy allocation, considering resource availability, demand, and grid reliability. When compared to CC and LF, ECD attained the lowest levelized cost of \$0.148/kWh and a net present cost of \$1.99 million through significant reductions in CO_2, CO, SO_2, and NOx emissions. The study primarily examined the operational aspects of the hybrid systems, excluding economic and decision-making considerations.

This study examines the viability of hybrid renewable energy systems integrating solar PV, wind turbines, batteries, and hydrogen storage for rural healthcare institutions in sub-Saharan Africa. Although hybrid systems for healthcare facilities have been the subject of earlier research, this study stands out by performing in-depth techno-economic analysis for two specific cases in South Africa and Nigeria. Additionally, the study assesses how various solar tracking configurations affect the viability and performance of the hybrid systems, offering fresh perspectives on optimizing renewable energy sources. In addition, this study utilizes a multi-criteria decision-making (MCDM) approach called the EDAS method to evaluate the trade-offs between various tracking configurations and system parameters. The environmental benefits and alignment of the proposed systems with the Sustainable Development Goals (SDGs) and climate change mitigation efforts are also discussed, emphasizing the innovative and significant nature of this research.

Materials and methods

This section outlines the strategy employed to accomplish the research objective. It describes the different steps used in the HOMER software to simulate the proposed hybrid renewable energy system (HRES). The proposed energy system consists of solar PV, wind turbines, batteries, fuel cells, and hydrogen tanks (Fig. 1). The methodology utilized in this study is unique in a variety of respects. The hybrid system designs examined in this study combine a unique mix of technologies, such as solar PV, wind turbines, batteries, and hydrogen storage. In addition, the research considered various solar tracking configurations (NT, HADA, HAMA, HAWA, TA, VACA, HACA) to assess their potential impact on the system's performance. Furthermore, the EDAS method is utilized for MCDM analysis, offering an alternative perspective on assessing the trade-offs among various system parameters and tracking configurations. This comprehensive methodology allows for a full evaluation of the practicality and improvement of hybrid renewable energy systems for healthcare facilities in remote areas.

Hybrid optimization of Multiple Energy Resources

This study utilized the Hybrid Optimization of Multiple Energy Resources (HOMER) software to conduct a techno-economic assessment of the solar PV/wind/battery/fuel cell off-grid hybrid renewable energy system (HRES). HOMER is a software program developed at the National Renewable Energy Laboratory to design and optimize microgrids. The HOMER enables the users to simulate a variety of components, including renewable sources, fossil-powered generators, energy storage systems, and loads [11]. The HOMER can assist in identifying the most cost-effective and reliable energy configurations through system optimization. Its features include renewable energy integration assessment, load analysis, sensitivity analysis, and economic assessment. Although the HOMER software is the primary tool utilized in this study to assess performance and optimize the design of the proposed hybrid renewable

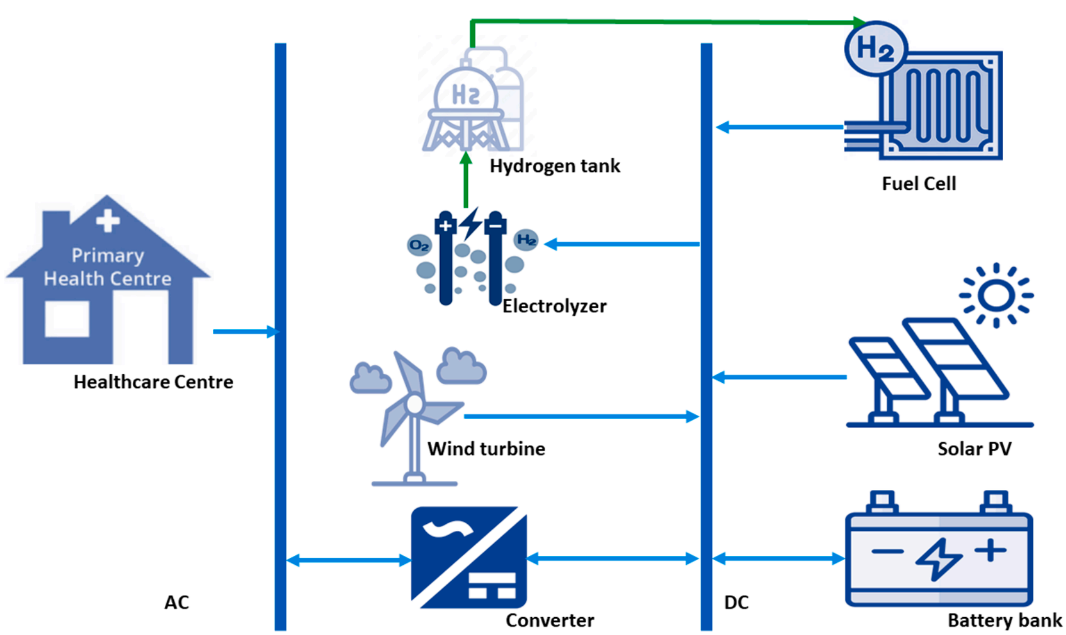

Fig. 1. Proposed hybrid renewable energy system for the healthcare clinic.

energy system. It is critical to recognize that there are additional optimization techniques that have been implemented in the literature. Optimization algorithms such as evolutionary algorithm [32] Mayfly Algorithm, Genetic Algorithm (GA), CUKO Search [31] Gray Wolf, Constrained Particle Swarm Optimization (CPSO) [43], Harmony Search (HS), cultural algorithm (CA) [46], artificial bee colony algorithm [35], and Flower Pollination Algorithm (FPA) have been deployed for HRES in the literature. These techniques offer unique advantages in terms of solution space exploration, convergence speed, and the ability to handle complex constraints.

However, this study selected HOMER software due to its widely recognized features and specific suitability for the techno-economic analysis of hybrid renewable energy systems. The evaluation of various system configurations and identifying optimal solutions are made more accessible by HOMER's user-friendly interface [7], large component libraries, and robust optimization algorithms [44]. It is a valuable tool for evaluating the viability and effectiveness of hybrid systems in various scenarios due to its capacity to carry out sensitivity assessments and consider various technical and economic factors [16].

Renewable energy resources

This study considers two locations in the African continent for implementing the proposed energy system. The study areas, i.e., Nigeria and South Africa solar resource data were acquired through the utilization of the HOMER's online retrieval system, which was connected to the NASA website. The variation of the solar resources in Nigeria (Akoka, Lagos) and South Africa (Phelandeba village, Eastern Cape), is presented in Fig. 2. It shows that the two locations have considerable solar resources. The daily average and the monthly solar irradiation and clearness indices of the locations are illustrated in Fig. 3. The mean daily solar irradiances in the South African and Nigerian locations are 4.97 kWh/m^2/day and 3.92 kWh/m^2, respectively. The maximum and minimum solar irradiation recorded in the South African location, are 6.41 kWh/m^2/day in the month of December and 3.55 kWh/m^2/day in the month of June, respectively. For the Nigerian location, the maximum and minimum solar irradiations are recorded in the month of July (5.99 kWh/m^2/day) and in the month of December (1.75 kWh/m^2/day). Furthermore, the clearness index fluctuated monthly from 0.306 in the month of June to 1.815 in the month of December in the South African location and between 0.465 (the month of January) and 0.535 (in the month of September) in the Nigerian location.

Fig. 4 presents the monthly average wind speeds (in meters per second) for the two locations, South Africa (SA), and Nigeria (NG). In the month of January, SA records an average wind speed of 5.88 m/s, whereas NG experiences an average speed wind of 2.835 m/s. The values fluctuate across the months, reflecting the dynamic nature of the wind patterns at the 2 locations. Notably, the month of June experiences a substantial increase in SA with an average wind speed of 10.95 m/s, while in NG the average wind speed peaks at 4.218 m/s in the month of May. These variations are crucial for assessing the wind energy potential that informs the decisions that are related to renewable energy projects, highlighting the importance of understanding the regional wind speed patterns for the effective planning and utilization of wind resources throughout the year.

Load demand

In assessing the resilience of the proposed HRES, this research was centered on a typical primary healthcare load profile. The load profile for the healthcare centre was obtained from the literature [13]. The medical equipment used in the healthcare centre, includes the: Refrigerator-vaccine (RV), Hematology analyzer (HA), Blood chemical analyzer (BCA), Refrigerator-nonmedical (RNM), Centrifuge, Microscope, and a CD4 Machine. Other non-medical equipment, includes lighting, radio, and functional desktop computers. The energy demand of the PHC is calculated by summing the individual electrical-consuming appliances' power by using Eq. (1) [10].

$$E_d = \sum_{f \in F} N_e \times \left(\sum_{e \in E} N_{ef} P_{ef} t_{ef} \right) \tag{1}$$

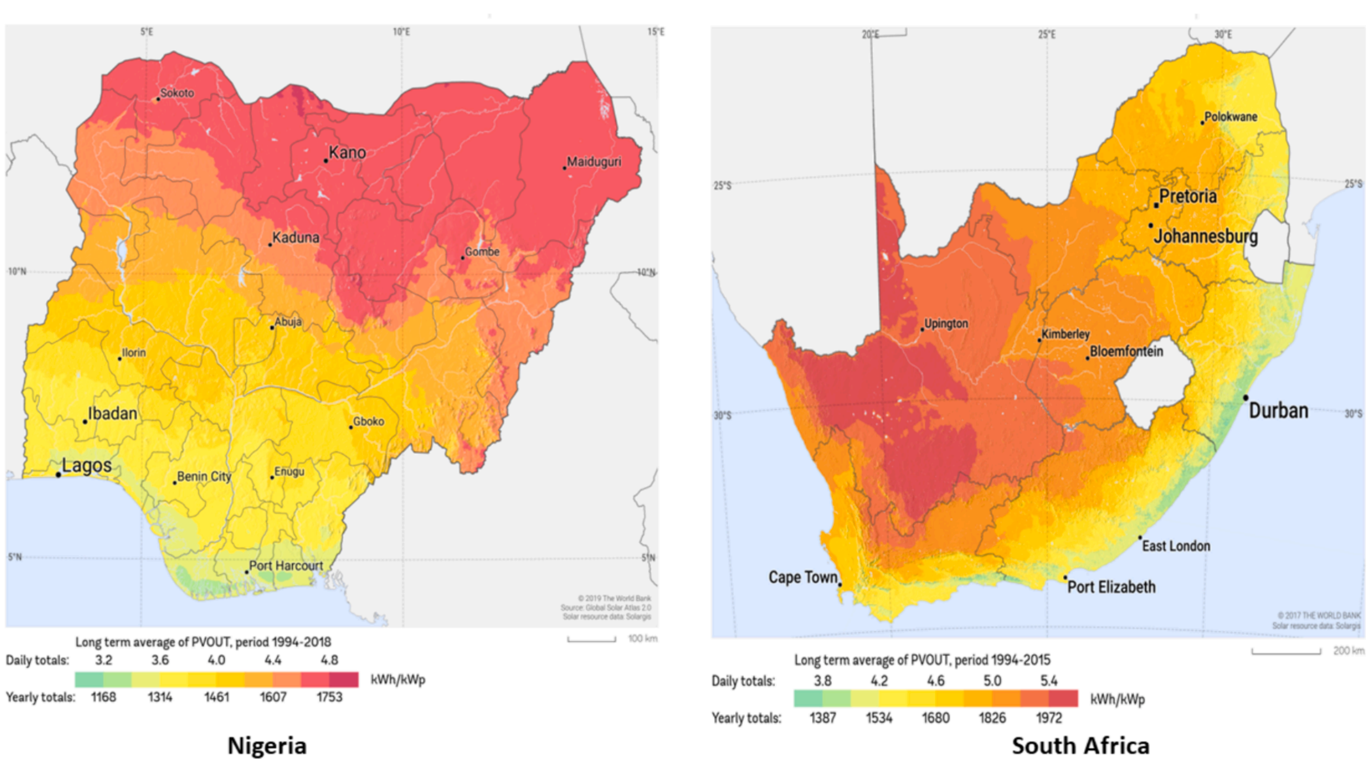

Fig. 2. Solar resource maps for Akoka, Lagos Nigeria, and Phelandeba village, Eastern Cape South Africa.

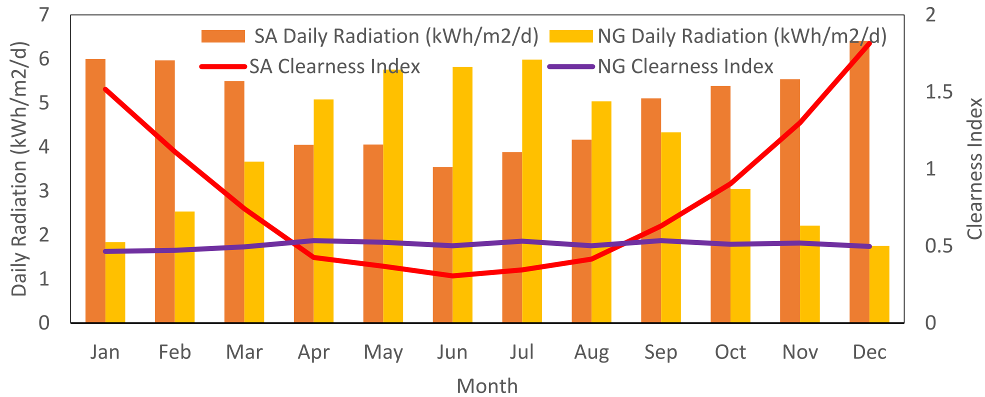

Fig. 3. Solar radiation and clearness indices Akoka, Lagos Nigeria and Phelandeba village, Eastern Cape South Africa.

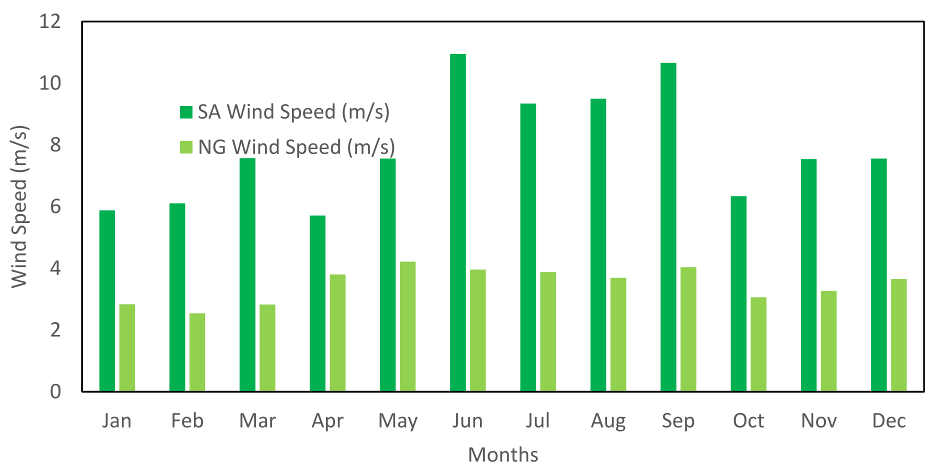

Fig. 4. Wind Speeds for South Africa and Nigeria.

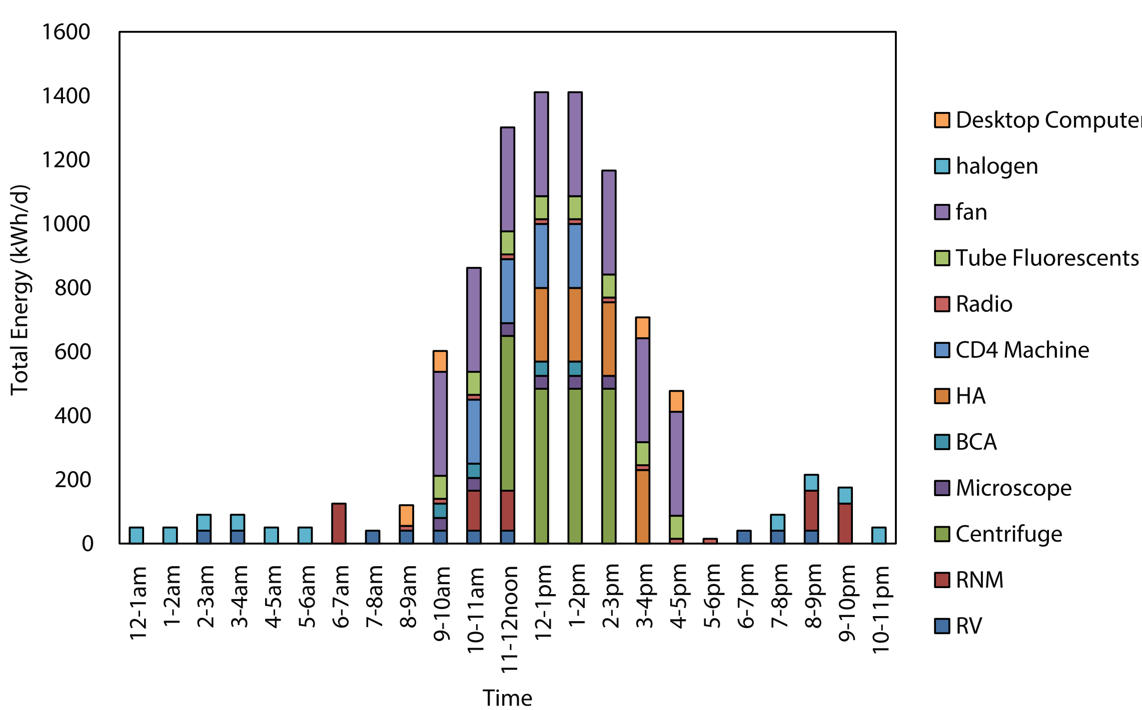

Fig. 5. Daily load profile showing the hourly consumption of the healthcare facility for a typical day.

the variable, e represents the specific type of equipment or appliance, such as: lighting, heating, refrigerating, or cooling. The variable, f represents the class, such as: commercial, agricultural, industrial, or educational of the equipment. N_e represents the total count of users, belonging to class e. N_{ef} represents the quantity of equipment that is associated with a particular class. P_{ef} represents the designated electrical power capacity of a certain equipment, e within the class, f, while t_{ef} denotes the total period of usage for each equipment, e within the class f. The typical duration of usage ranges between minutes to hours.

Shown in Fig. 5 is the daily load profile, showing the hourly consumption of the healthcare facility for a typical day in a week. The examination of the pattern of usage during hospital operations reveals a consistent baseline load of ~ 0.1 kWh during the nighttime period, i.e., from midnight to 6 am. This load is mostly due to the refrigeration needs and the continuous operation of the lighting facilities. The usage shows a significant increase, starting at 8 am, coinciding with the commencement of the clinic's operating hours. The highest level of electricity consumption occurs between mid-morning and noon, namely during the active patient testing and treatment operations. The range of electricity usage during this period is between 0.933 kWh and 1.599 kWh per hour. In the evening, when activity decreases, the energy consumption rapidly decreases and returns to the overnight baseline of 0.1 kWh; the daily average consumption is 12.5 kWh/day.

System configuration

This section discusses the technical and economic specifications and models adopted in this study. The technical and economic parameters are essential in designing a hybrid renewable energy system for a healthcare institution, which is presented in Table S1. Each component, including PV panels, batteries, wind turbines, fuel cells, Electrolyzers, hydrogen tanks, and converters, has specific rated capacities, capital costs, replacement costs, O&M expenses, and lifespans. In this study, the PV panels used have a power output of 0.25 kW and have a capital cost of $295 with a lifespan of 20 years. On the other hand, the battery has a voltage rating of 12 V and a capacity of 200Ah. It costs $357 and has a lifespan of 4 years. The Fuel Cell has a power output of 1 kW, a capital cost of $4000, and a lifespan of 40,000 h. The Electrolyzer under consideration has a capacity of 8 kW and a capital cost of $2700, with an annual operating and maintenance cost of $3. The Electrolyzer has a lifespan of 15 years. The wind turbine has a power rating of 0.4 kW (DC) and costs $465 to install. Its annual operation and maintenance cost is $5, and it has a lifespan of 15 years. The Hydrogen Tank is essential for storing hydrogen generated by the Electrolyzer; it has a capacity of 8 kg, a capital cost of $3100, and a lifespan of 25 years. Finally, the Converter has a rated capacity of 1 kW, a capital cost of $37, and a lifespan of 10 years.

Solar photovoltaic

Photovoltaic (PV) technology operates by directly converting sunlight into electricity by using PV modules [2]. PV modules, or solar panels, are created by physically and electrically connecting solar cells and placing them within a frame. The power output of a photovoltaic (PV) module depends on both the specific technology of the module and the level of solar irradiance it receives. The power generated by a module at a specific moment is directly proportional to the perpendicular intensity of sunlight on the surface of the module [36]. The HOMER employes Eq. (2) to determine the PV panel's power output.

$$P_{pv} = Y_{pv} f_{pv} \left(\frac{\overline{G_T}}{\overline{G_{T,STC}}} \right) \left[1 + \alpha_P \left(T_C - T_{C,STC} \right) \right] \tag{2}$$

$$T_c = \left(\frac{T_a + \left(T_{c,NOCT} - T_{a,NOCT} \right) \left(\frac{G_T}{G_{T.STC}} \right) \left(\frac{\left[1 - \eta_{mp,STC} \left(1 - \mu \cdot T_{cSTC} \right) \right]}{\alpha \tau} \right)}{1 + \left(T_{c,NOCT} - T_{a,NOCT} \right) \left(\frac{G_T}{G_{T.STC}} \right) \left(\frac{\mu_m \eta_{mp,STC}}{\alpha \tau} \right)} \right) \tag{3}$$

whereY_{pv} is the rated capacity of the PV array ,f_{pv} is the PV de-rating factor (%), $\overline{G_T}$ is the solar irradiation incident on the PV array (kW/m^2) ,$G_{T,STC}$ is the solar irradiation incident in a standard condition $(1kW/m^2)$, α_P is the temperature coefficient of power $(\%/^{\circ}C)$, T_C is the PV cell temperature $(^{\circ}C)$, $T_{C,STC}$ is the PV cell temperature under standard test conditions $(^{\circ}C)$. $T_{a,NOCT}$ and $T_{c,NOCT}$ represent the cell surface temperature at nominal and actual conditions in degrees Celsius, respectively. $\eta_{mp,STC}$ indicates the efficiency of the solar system at maximum power output. α is the PV array's solar absorptance (%) and τ is the solar transmittance of any cover, over the PV array (%). The derating fact for the PV panel is taken as 90 %, ground reflectance as 20 %, temperature coefficient of power as −0.5 %/C, nominal operating cell temperature is taken as 47 °C and the efficiency at standard test condition is 13 %.

Solar photovoltaic (PV) tracking

Solar PV tracking enables solar panels to dynamically align with the sun's position during the day, resulting in enhanced energy capture, in comparison to the stationary tilt systems. The solar tracking configurations [11] that were considered in this study, include:

i. *No Tracking (NT):* Solar panels are stationary and do not follow the sun's path; it is the simplest and least expensive choice since it uses the least amount of energy.
ii. *Horizontal Axis, Monthly Adjustment (HAMA*): The tilt angle of the panels is manually adjusted once a month to align with the sun's seasonal angle. The panels rotate on a horizontal north–south axis.
iii. *Horizontal Axis, Weekly Adjustment (HAWA):* The horizontal axis remains constant, while the tilt angle is modified on a weekly basis. It enhances energy acquisition in comparison to a monthly adjustment scenario but necessitates more frequent manual adjustments.
iv. *Horizontal Axis, Daily Adjustment (HADA):* The panels undergo horizontal rotation, and their tilt is automatically adjusted daily to align with the sun's angle. The energy capture is greatly enhanced, however, the costs associated with the system and its maintenance also experience a notable increase.
v. *Horizontal Axis, Continuous Adjustment (HACA*): Panels tilt and rotate continually on a horizontal axis to precisely track the location of the sun throughout the day.
vi. *Vertical Axis, Continuous Adjustment (VACA):* The panels rotate around a vertical axis to follow the sun's movement from east to west, but they do not adjust their angle to match the sun's altitude.
vii. *Two-Axis Tracking (TA*): The panels can rotate separately along both the horizontal and vertical axes to accurately track the sun's location in any direction. It optimizes the energy collection, while simultaneously maximizing the system complexity and expenses.

Wind turbine

Wind turbines generate electricity by utilizing the velocity of the air to rotate a set of blades. The power produced by a wind turbine is dependent on various factors, such as: the wind speed, the length of the blades, and the wind turbine power coefficient, which characterize the efficiency with which, the turbine transforms wind energy into rotational motion. Eqs. **(4) and (5)** provide a method for the estimation of the output of a wind turbine [3]. Three stages are required for the HOMER to calculate the power output of a wind turbine. They are:

1. The hourly wind speed is modified from the anemometer height to the hub height through the utilization of the logarithmic profile or the power law.

$$V_h = V_m \times \left(\frac{H_h}{H_m}\right)^{\beta} \tag{4}$$

2. The next step entails the estimation of the power produced under standard conditions (pressure and temperature) by referencing the power curve of the specified wind turbine.
3. The last step involves the multiplication of the values obtained in the second step by the air density to determine the wind power output.

$$P_o = P_{o,STP} \times \frac{\rho}{\rho_o} \tag{5}$$

The wind speed at the proposed hub height, H_h is denoted as V_h, while V_m represents the wind speed, measured at height H_m, where the anemometer is located for the wind speed measurement, β is the power law exponent (usually taken as 1/7 [33]), ρ is the real density of air, and ρ_o is the density of air at standard temperature and pressure. $P_{o,STP}$ refers to the output of the wind turbine at standard temperature and pressure.

Fuel cell

The fuel cell, electrolyzer, and hydrogen storage tank make up the hydrogen energy system [34]. The equation for the calculation of the rate of hydrogen production in an electrolyzer is provided in Eq. (8). The hydrogen generated by this procedure is pressurized and stored in a hydrogen reservoir. The energy required [9] to compress the hydrogen gas, is represented in Eq. (6). The fuel cell is utilized to transform the stored hydrogen into electrical energy, and the power generated by a fuel cell may be determined [9] by using Eq. (7).

$$\propto \dot{H}_2 = \eta_f \left(\frac{I_e \times N_s}{n \times F}\right) \tag{6}$$

$$P_{com} = \eta_f \left(\frac{I_e \times N_s}{n \times F}\right) \times \left[\left(\frac{P_2}{P_1}\right)^{\frac{\gamma-1}{\gamma}}\right] \times \left(\frac{\gamma - 1}{\gamma}\right) \times \left(\frac{T}{\eta_{com}}\right) R \tag{7}$$

$$FC_{ele} = LHV_h \times \propto \dot{H}_2 \times \rho_h \times \eta_{fc} \tag{8}$$

HOMER is an energy simulation software with a powerful integrated approach in modeling the performance of fuel cell systems, either separately or coupled with electrolyzers. In modeling fuel cell energy production, HOMER regards the fuel cells as DC generators. Users can define the fuel source as either stored hydrogen produced by an electrolyzer or use an externally-supplied fuel that is reformed. In the latter case, the generator module satisfies both the reformer and fuel cell while factoring in the costs and efficiency curve on a combined basis. For electrolyzer energy consumption, HOMER uses a simplified model that assumes constant efficiency: a fixed amount of electricity input will give a given amount of hydrogen output. HOMER simulates electrolyzer by assuming constant efficiency, meaning that a specific quantity of power will consistently produce a specific quantity of hydrogen. The electrolyzer has a specified minimum load level, meaning it can only function at a capacity as low as 75 % of its maximum rating. Therefore, there is the option to adjust the minimum load setting to match this threshold of 75 %. However, when hydrogen is required for a load or generator, the electrolyzer will demand electricity. HOMER calculates fuel cell efficiency based on input fuel consumption data and allows users to enter specific fuel cell or electrolyzer data into its fuel curve calculator for more precise modeling.

Storage capacity

The quantity of batteries required for the energy system is determined by using Eq. (9), while the capacity of the hydrogen tank, $\boldsymbol{C_{h,tank}}$, is calculated as the quotient of the load demand and the energy content, as described (Babatunde et al., 2022) in Eq. (10).

$$n_b = \frac{Batt_{aut} \times E_b(1000/kWh)}{V_n Q_n \left(\frac{100 - SOS_{min}}{100}\right)(24hr/day)} \tag{9}$$

$$C_{h,tank} = \frac{H_{aut} \times E_d\left(\frac{3.6MJ}{kWh}\right)}{LHV_h(24hr/day)} \tag{10}$$

$Batt_{aut}$ represents the battery autonomy, $\boldsymbol{SOS_{min}}$ represents the minimum state of charge of the battery (%), $\boldsymbol{Q_n}$ represents the nominal capacity of a single battery (in Ah), $\boldsymbol{V_n}$ represents the nominal voltage of a single battery (in V), n_b represents the number of batteries, $\boldsymbol{H_{aut}}$ represents the autonomy of the hydrogen tank, and LHV_h represents the energy content (lower heating value) of hydrogen, which is 120 MJ/kg.

Battery lifetime throughput

Battery lifetime throughput refers to the total amount of energy that a battery can deliver or store over its entire operational lifespan. It is a crucial metric in evaluating the performance and durability of a battery, especially in applications where the battery's energy storage capacity and cycle life are essential factors. Tracking battery lifetime throughput helps assess the efficiency and reliability of the battery in meeting the energy demands of a particular system or device. HOMER assumes that a fixed amount of energy can be cycled through a battery before it requires replacement, regardless of the depth of the individual cycles. HOMER calculates a value of lifetime throughput ($\boldsymbol{Q_{lifetime,i}}$) using the following equation:

$$Q_{lifetime,i} = f_i d_i \left(\frac{V_n \times q_{max}}{1000W/kW}\right) \tag{11}$$

where d_i is the depth of discharge (%) f_i is the number of cycles to failure, and q_{max} is the maximum capacity of the battery [Ah].

Control strategies

Considering the multi-source nature of the proposed energy system, it is necessary to implement an operational strategy to effectively coordinate the flow of energy among the different components. This study did implement two dispatch strategies, *viz*: load following the load following (LF) and the cycle-charging (CC) strategies [11]. A dispatch strategy refers to a set of rules or actions implemented to regulate the functioning of the energy sources and storage components, particularly, when the power generated by renewable energy sources is inadequate to satisfy the demand. The load-following technique involves the power plant producing sufficient energy to meet the load requirements while the storage devices remain unchanged. In the cycle-charging mode, the generator operates at its maximum rated capacity to meet the load requirements and recharge the storage system with any surplus energy.

Cost models

The cost models used for evaluating the renewable energy systems' economic viability are discussed in this section. These include the Total Net Present Cost and the Levelized Cost of Energy.

Total net present cost

The total net present cost (TNPC) of a system is calculated by subtracting the present value of all the revenue it generates over its lifetime from the present value of all the costs it incurs over its lifetime. The costs encompass the capital expenditures, expenses for replacement, operation and maintenance, fuel expenditures, penalties for pollution, and the expenses associated with current the purchase of electricity from the grid. Revenues consist of the value obtained from salvage and the revenue generated from grid sales. By using Eq. (12), the HOMER model can estimate the total net present cost.

$$TNPC = \frac{TC_{ann}}{F_{cr}(i,X_{proj}} \tag{12}$$

where, TC_{ann} is the total annual cost incurred, while F_{cr} is the capital recovery factor. i is the interest rate (in %) and X_{proj} represents the project lifespan. This work adopted i as 12 % and X_{proj} to be 25 years.

Levelized cost of energy (LCOE)

The levelized cost of energy (COE) is defined by the HOMER model as the average cost per kilowatt-hour (kWh) of the productive electrical energy generated by the system. The HOMER utilizes the ratio of the yearly cost of electricity production (subtracting the cost of feeding the thermal load) to the total useable electric energy production i to determine the COE. For this case study, the HOMER employed Eq. (13) to calculate the COE.

$$LCOE = \frac{TC_{ann}}{TDEM} \tag{13}$$

where $TDEM$ is the total amount of electricity demand that was supplied by the source of electricity generation.

Evaluation based on distance from average solution method

Evaluation based on Distance from Average Solution, or EDAS, is a technique applied to study the optimization and the multi-criteria decision-making (MCDM) problems [12]. It assists in assessing and prioritizing the available alternatives according to how close they are to the average solution. The goal of EDAS is to identify solutions that are both close to the average and have high individual performance across multiple criteria. The distance calculation uses a normalized Euclidean distance metric. Assuming there are n alternatives and m criteria, the EDAS method can be implemented [23] by using the following steps.

Step 1: Select the evaluation criteria for a decision-making problem.

Step 2: Design a decision-making matrix by using the selected criteria.

Step 3: Determine each criterion's average solution.

Step 4: Formulate the PDA and NDA matrices for the evaluation process.

Step 5: Generate the alternatives' weighted sums of *PDA* and *NDA*.

Step 6: Normalize the alternatives' *SP* and *SN* values.

Step 7: Determine the alternatives' appraisal score (*AS*).

Step 8: Rank the alternatives, based on their appraisal scores by using the higher, the better concept.

Assumptions, Limitations, and uncertainties

The study assumes that the solar radiation and wind speed data from the NASA database accurately reflect the long-term averages for the specific areas in Nigeria and South Africa selected for the case study. Also, the study applied a day-to-day and time-step-to-time-step random variability of 10 % to load demand. It is assumed that the randomness would make the load profile more practical and capture the seasonal variations. Furthermore, system component technical specifications and costs are based on current market data and remain relatively constant. Economic parameters are also assumed to be stable over the project duration, and the HOMER software's optimization algorithms and calculations are presumed to be accurate and reliable.

The study is limited by its reliance on secondary data sources, its focus on two specific locations that may not be generalizable to other regions, and the exclusion of social, cultural, and institutional factors that may affect implementation and adoption. HOMER software's optimization results are based on the specific input parameters and assumptions used in the study, and variations in these inputs may lead to different optimal system configurations and techno-economic outcomes. Hence, it is proposed that future studies consider the effects of change in input parameters on the study's outcome. This study does not consider the social, cultural, and institutional aspects of hybrid renewable energy system acceptance and implementation in rural healthcare institutions.

Furthermore, the results of this study are based on the assumption that batteries would be replaced once it reaches its lifetime throughput, as calculated by HOMER using Eq. (11). However, it is important to note that our analysis does not include a detailed battery degradation model. Battery degradation happens because of different things like temperature, depth of discharge, and charging/discharging rates [40]. As the battery degrades, its capacity and performance decrease; this would mean they need to be replaced more often and spend more. Future work is expected to focus on integrating a detailed battery lifetime model that captures the effects of degradation on the system's performance and economic viability. This could involve using empirical data or physics-based models to predict the battery's capacity fade and resistance increase over time. By incorporating a more realistic battery degradation model, future studies can provide more accurate and reliable insights into the feasibility and cost-effectiveness of hybrid renewable energy systems for rural healthcare facilities.

Despite these limitations and uncertainties, this study provides valuable insights into the feasibility and potential of hybrid renewable energy systems for rural healthcare facilities in sub-Saharan Africa. The results can serve as a basis for further detailed engineering design, pilot projects, and policy development to support the implementation of sustainable energy solutions in the healthcare sector.

Results and discussion

This section discusses the results of the techno-economic simulation of the proposed energy system for healthcare centers and the MCDM assessments for the various tracking systems. The simulation results for the Nigerian and South African cases are presented in Tables 1 and 2, respectively. The techno-economic details of the battery bank connected to the optimal energy systems are presented in Tables S2 and S3.

Nigeria

The techno-economic results of the viable energy systems for the seven tracking configurations for the Nigeria case study is presented in this section.

No-tracking

The optimal non-tracking energy system for the PHC in Lagos employs a 5 kW solar photovoltaic (PV) array as the primary power source, supplemented by a 10 kW fuel cell and a 10 kW inverter to power the system when solar power is unavailable. An electrolyzer with a power capacity of 10 kW, a rectifier with a power capacity of 7.5 kW, and a hydrogen tank, weighing 16 kg allow for the storage of the solar PV power as hydrogen, which may be utilized later in the fuel cell. The system's lifetime net present cost amounted to $14,272, whereas the levelized cost of energy was $0.336/kWh. The photovoltaic (PV) array accounted for 90 % of the annual power production with a capacity factor of 15 %. The implementation of the tracking mechanisms to

Table 1
Techno-economic results of the proposed energy system with and without a solar tracking scenario for Nigeria.

	Rank	PV (kW)	wind turbine (No)	Fuel cell (kW)	Battery (No)	Converter (kW)	Electrolyzer (kW)	Hydrogen Tank (kg)	Total NPC ($)	COE ($/kWh)	Tot. Electrical production (kWh/yr)	Cap. Shortage (kWh/yr)	Unmet Load (kWh/ yr)	Excess Electricity (kWh/yr)	NOx Emissions (kg/yr)	Battery Autonomy (hr)	Battery Throughput (kWh/yr)	hydrogen tank autonomy (hours)	Total hydrogen production (kg/yr)	LCOH ($
NT	1	5	0	10	0	10	10	16	14,272	0.34	7,263	30	24	1,136	2	0	0	1396	53.4	21
	2	5	1	10	0	10	10	12	14,617	0.34	7,335	34	28	1,457	2	0	0	1047	48.1	24
	3	5	0	10	10	10	10	3	14,711	0.34	6,824	4	3	2,255	1	37.69	461	262	16.6	69
	4	5	2	0	10	10	0	0	15,321	0.36	6,772	30	24	2,960	0	37.69	604	0	0	0
	5	5	1	10	10	10	10	3	15,338	0.36	6,913	1	1	2,390	1	37.69	430	262	15.7	76
	6	5	0	0	15	10	0	0	17,191	0.4	6,552	27	22	2,729	0	56.53	679	0	0	0
HADA	1	5	0	10	0	10	10	12	14,612	0.34	7,556	33	27	1,567	2	0	0	1047	50.5	23
	2	5	1	10	0	10	10	8	14,953	0.35	7,628	37	30	1,888	2	0	0	698	45.2	26
	3	5	0	10	10	10	10	3	15,135	0.35	7,129	3	2	2,517	1	37.69	457	262	17.6	67
	4	5	2	0	10	10	0	0	15,722	0.37	7,062	31	25	3,248	0	37.69	613	0	0	0
	5	5	1	10	10	10	10	3	15,755	0.37	7,218	0	0	2,652	1	37.69	428	262	16.7	74
	6	5	0	0	15	10	0	0	17,593	0.41	6,842	24	20	3,013	0	56.53	689	0	0	0
HAMA	1	5	1	10	10	10	10	28	16,103	0.38	6,255	37	29	1,000	1	37.69	401	2443	32.8	39
	2	5	0	10	15	10	10	28	18,674	0.44	6,157	34	27	901	1	56.53	437	2443	32.8	45
	3	10	0	10	0	10	10	2	20,717	0.48	12,398	0	0	7,079	2	0	0	174	35.1	46
	4	10	0	0	10	10	0	0	21,088	0.49	11,827	0	0	7,995	0	37.69	519	0	0	0
	5	10	1	10	0	10	10	2	21,138	0.49	12,480	0	0	7,223	2	0	0	174	33.7	49
	6	10	1	0	10	10	0	0	21,753	0.51	11,937	0	0	8,113	0	37.69	480	0	0	0
HAWA TA	1	5	0	10	10	10	10	28	15,360	0.36	6,345	33	27	907	1	37.69	455	2443	36	33
	2	5	1	10	10	10	10	24	15,938	0.38	6,422	34	28	1,197	1	37.69	427	2094	31.6	40
	3	10	0	10	0	10	10	2	20,706	0.48	12,618	0	0	7,292	2	0	0	174	35.2	46
	4	10	0	0	10	10	0	0	21,088	0.49	12,049	0	0	8,217	0	37.69	518	0	0	0
	5	10	1	10	0	10	10	2	21,129	0.49	12,700	0	0	7,436	2	0	0	174	33.9	49
	6	10	1	0	10	10	0	0	21,753	0.51	12,159	0	0	8,335	0	37.69	480	0	0	0
	1	5	0	10	0	10	10	3	15,113	0.36	8,810	36	29	3,199	2	0	0	262	42.4	28
	2	5	1	10	0	10	10	3	15,524	0.37	8,889	32	26	3,344	2	0	0	262	40.9	30
	3	5	1	0	10	10	0	0	15,695	0.37	8,215	30	24	4,396	0	37.69	632	0	0	0
	4	5	1	10	10	10	10	0	15,743	0.37	8,215	30	24	0	0	37.69	632	0	94.7	13
	5	5	0	10	10	10	10	3	15,800	0.37	8,405	0	0	3,751	1	37.69	442	262	18.6	67
	6	5	0	0	15	10	0	0	18,230	0.43	8,105	16	13	4,267	0	56.53	692	0	0	0
VACA	1	5	3	10	10	10	10	28	17,207	0.41	6,907	35	28	1,659	1	37.69	384	2443	32.5	42
	2	10	0	10	0	10	10	2	20,563	0.48	13,304	0	0	7,996	2	0	0	174	34.8	46
	3	10	0	0	10	10	0	0	20,980	0.49	12,738	0	0	8,906	0	37.69	516	0	0	0
	4	10	1	10	0	10	10	2	20,992	0.49	13,387	0	0	8,140	2	0	0	174	33.5	49
	5	10	0	10	10	10	10	0	21,028	0.49	12,738	0	0	0	0	37.69	516	0	192	8.6
	6	10	1	0	10	10	0	0	21,645	0.51	12,847	0	0	9,024	0	37.69	478	0	0	0
HACA	1	5	2	0	10	10	0	0	16,229	0.38	7,206	33	26	3,394	0	37.69	612	1047	50.3	24
	2	5	0	0	15	10	0	0	18,100	0.43	6,986	26	21	3,160	0	56.53	687	1047	49	25
	3	5	0	10	10	10	10	3	53,751	1.26	7,086	8	6	2,905	0	37.69	701	262	17.6	70
	4	5	2	10	10	10	10	0	53,983	1.27	7,206	33	26	0	0	37.69	612	0	0	0
	5	5	3	10	0	10	10	6	90,763	2.14	7,950	35	28	2,374	2	0	0	262	16.7	76
	6	10	0	10	0	10	10	2	94,593	2.21	14,539	0	0	9,188	2	0	0	0	0	0

Table 2
Techno-economic results of the proposed energy system with and without a solar tracking scenario for South Africa.

	Rank	PV (kW)	wind turbine (No)	Fuel cell (kW)	Battery (No)	Converter (kW)	Electrolyzer (kW)	Hydrogen Tank (kg)	Total NPC ($)	COE ($/kWh)	Tot. Electrical production (kWh/yr)	Cap. Shortage (kWh/yr)	Unmet Load (kWh/ yr)	Excess Electricity (kWh/yr)	NOx Emissions (kg/yr)	Battery Autonomy (hr)	Battery Throughput (kWh/yr)	hydrogen tank autonomy (hours)	Total hydrogen production (kg/yr)	LCOH ($/kg)
NT	1	5	0	10	0	10	10	16	14,272	0.336	7,263	30	24	1,136	2	0	0	1.396	53.4	20.9
	2	5	1	10	0	10	10	12	14,617	0.344	7,335	34	28	1,457	2	0	0	1.047	48.1	23.8
	3	5	0	10	10	10	10	3	14,711	0.344	6,824	4	3	2,255	1	37.69	461	262	16.6	69.2
	4	5	2	0	10	10	0	0	15,321	0.361	6,772	30	24	2,960	0	37.69	604	0	0	0
	5	5	1	10	10	10	10	3	15,338	0.359	6,913	1	1	2,390	1	37.69	430	262	15.7	76.2
	6	5	0	0	15	10	0	0	17,191	0.404	6,552	27	22	2,729	0	56.53	679	0	0	0
HADA	1	5	0	0	10	10	0	0	14,393	0.339	8,390	31	27	4,533	0	37.69	755	0	0	0
	2	5	0	10	10	10	10	0	14,441	0.34	8,390	31	27	0	0	37.69	755	0	97.7	11.6
	3	5	0	10	0	10	10	2	14,448	0.34	9,160	24	20	3,287	3	0	0	174	48	23.6
	4	5	1	10	0	10	10	2	14,993	0.351	9,246	9	7	3,409	3	0	0	174	46.9	25
	5	5	1	0	10	10	0	0	15,058	0.354	8,494	24	21	4,640	0	37.69	711	0	0	0
	6	5	1	10	10	10	10	0	15,106	0.355	8,494	24	21	0	0	37.69	711	0	100	11.8
HAMA	1	5	0	0	10	10	0	0	14,393	0.339	5,963	30	26	2,100	0	37.69	797	0	0	0
	2	5	0	10	10	10	10	0	14,441	0.34	5,963	30	26	0	0	37.69	797	0	45.3	25
	3	5	0	10	0	10	10	3	14,760	0.346	6,781	16	14	853	3	0	0	262	49.1	23.5
	4	5	1	0	10	10	0	0	15,058	0.354	6,067	23	20	2,207	0	37.69	751	0	0	0
	5	5	1	10	10	10	10	0	15,106	0.355	6,067	23	20	0	0	37.69	751	0	47.6	24.8
	6	5	1	10	0	10	10	3	15,268	0.358	6,859	8	7	976	3	0	0	262	48	24.9
HAWA	1	5	0	0	10	10	0	0	14,393	0.339	6,229	30	26	2,368	0	37.69	791	0	0	0
	2	5	0	10	10	10	10	0	14,441	0.34	6,229	30	26	0	0	37.69	791	0	51	22.1
	3	5	0	10	0	10	10	2	14,672	0.345	7,031	28	24	1,145	3	0	0	174	48.4	23.7
	4	5	1	0	10	10	0	0	15,058	0.354	6,334	23	20	2,475	0	37.69	746	0	0	0
	5	5	1	10	10	10	10	0	15,106	0.355	6,334	23	20	0	0	37.69	746	0	53.3	22.2
	6	5	1	10	0	10	10	2	15,213	0.357	7,117	12	10	1,250	3	0	0	174	47.6	25
TA	1	5	0	0	10	10	0	0	15,030	0.354	10,470	28	24	6,611	0	37.69	754	0	0	0
	2	5	0	10	10	10	10	0	15,078	0.355	10,470	28	24	0	0	37.69	754	0	142	8.28
	3	5	0	10	0	10	10	2	15,149	0.355	11,253	6	5	5,330	3	0	0	174	48.7	24.3
	4	5	1	10	0	10	10	2	15,646	0.366	11,330	0	0	5,478	3	0	0	174	47	26
	5	5	1	0	10	10	0	0	15,695	0.369	10,575	22	18	6,719	0	37.69	709	0	0	0
	6	5	1	10	10	10	10	0	15,743	0.37	10,575	22	18	0	0	37.69	709	0	145	8.51
VACA	1	5	0	0	10	10	0	0	14,285	0.336	6,160	28	24	2,298	0	37.69	798	0	0	0
	2	5	0	10	10	10	10	0	14,333	0.337	6,160	28	24	0	0	37.69	798	0	49.5	22.6
	3	5	0	10	0	10	10	4	14,609	0.343	6,977	13	11	1,041	3	0	0	349	49.2	23.2
	4	5	1	0	10	10	0	0	14,950	0.351	6,264	21	18	2,405	0	37.69	752	0	0	0
	5	5	1	10	10	10	10	0	14,998	0.352	6,264	21	18	0	0	37.69	752	0	51.8	22.6
	6	5	1	10	0	10	10	4	15,075	0.353	7,048	12	10	1,183	3	0	0	349	47.6	24.8
HACA	1	5	0	0	10	10	0	0	14,900	0.351	8,507	31	26	4,650	0	37.69	753	0	0	0
	2	5	1	0	10	10	0	0	15,565	0.366	8,611	24	20	4,757	0	37.69	709	0	100	11.7
	3	5	0	10	10	10	10	0	52,654	1.24	8,507	31	26	0	0	37.69	753	174	48.4	24.2
	4	5	1	10	10	10	10	0	53,319	1.254	8,611	24	20	0	0	37.69	709	174	47	25.8
	5	5	3	10	0	10	10	2	89,772	2.098	9,521	0	0	3,816	2	0	0	0	0	0
	6	5	0	10	0	10	10	2	92,255	2.163	9,284	14	11	3,383	3	0	0	0	103	11.9

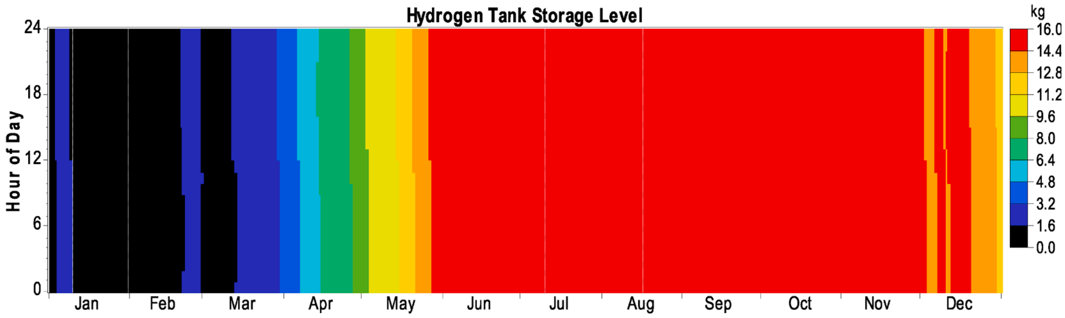

Fig. 6. Monthly hydrogen tank storage levels for the optimal energy system of a non-tracking configuration.

enhance the capacity factor can significantly increase the energy production of the photovoltaic systems. The fuel cell contributed 10 % of the power required to compensate for the periods when solar energy was inaccessible, however, functioned for more than 5,000 h annually. An analysis of the hydrogen tank storage level (Fig. 6) shows that hydrogen production peaked between the months of mid-May and early November when the wind speed and solar radiation are at their cumulative peaks. The capacity factor and efficiency of 50 % are acceptable. The annual un-met load was 24 kWh, whereas the excess power generation is ~ 1,100 kWh. The surplus electricity can be utilized to enhance the electrolyzer's capacity for increased hydrogen fuel production and improved reliability. The system effectively handled the load by using 100 % renewable energy. Because it is a renewable power set-up, emissions are significantly minimized. The fuel cell alone emitted only ~ 2.47 kg/year of nitrogen oxides.

Horizontal Axis, daily Adjustment

The most economical configuration of the HADA system comprises a 5 kW photovoltaic (PV) array, a 10 kW fuel cell, a 10 kW inverter, a 7.5 kW rectifier, a 10 kW electrolyzer, and a 12 kg hydrogen tank. The system had a total net present cost of $14,612, a levelized cost of energy of $0.344/kWh, and an annual operating cost of $624. The photovoltaic (PV) array represented 46 % of the system's expenditure, while the fuel cell constituted 44 %. The electricity production amounts to 7,556 kWh/yr, with photovoltaic (PV) systems contributing 91 % and fuel cells for the remaining 9 %. The primary load consumed 3,320 kWh/yr, which accounted for 59 % of the total energy consumption. The electrolyzer consumes 2,342 kWh annually, representing 41 % of the total energy consumption. The monthly hydrogen tank storage level for the optimal energy system for the HADA configuration is presented in Fig. 7.

The hydrogen level pattern for the HADA configuration also followed that without a tracking system, there is deficient production between the months of January and February, while the hydrogen level was highest between the months of May and December. Additionally, there was a surplus of 1,567 kWh/yr from renewable energy sources. The annual hydrogen output was 50 kg, while the consumption rate was 42.8 kg/yr. The hydrogen tank had a storage capacity of 1,047 h. The net CO_2 emissions were −0.438 kg/yr, indicating a negative value, and the annual emission of NOx was 2.48 kg.

Horizontal Axis, monthly Adjustment

An optimal configuration for the tracking of HAMA comprised a 5 kW photovoltaic (PV) array, a 1 kW wind turbine, a 10 kW fuel cell, a 10 kW battery bank, a 10 kW inverter, a 7.5 kW rectifier, a 10 kW electrolyzer, a 28 kg hydrogen tank, and a load following (LF) dispatch strategy. The system had a total net present cost of $16,103. It also had a levelized energy cost of $0.380 per kilowatt-hour and an annual operating cost of $425. The photovoltaic (PV) array represented 42 % of the system's overall cost, while the battery bank represented 40 %. The expenses that were related to the initial investment were 65 % of the system's overall expenditures. The overall electricity production amounted to 6,255 kWh per year, with the photovoltaic (PV) systems contributing 95 %, wind power contributing 2 %, and fuel cells contributing 4 %. The renewable energy surplus was 1,000 kWh annually, while the primary load consumed 3,318 kWh annually, accounting for 69 % of the total consumption. The electrolyzer consumed 1,520 kWh annually, accounting for 31 % of the total consumption. The tank had a storage capacity of more than 2,400 h, with hydrogen production at 33 kg per year and consumption at 13.9 kg per year. The monthly hydrogen tank storage level for the optimal energy system for the HAMA configuration showed low levels of hydrogen between the months of January and mid-March and high levels of storage between the months of mid-June and early December (Fig. 8). The battery connected to the HAMA system is projected to have a lifetime throughput of 9170 kWh during its 10-year lifespan, with an average annual energy output of 401 kWh (Table S2). Other technical and economic features of the battery is given in Table S2. The net CO_2 emissions were −0.142 kg/yr, indicating a reduction in the CO_2 levels. Additionally, there were 0.806 kg/yr of NOx emissions.

Horizontal Axis, weekly Adjustment

The optimal design for the HAWA tracking system includes a 5 kW PV array, a 10 kW fuel cell, a 10 kW battery bank, a 10 kW inverter, a 7.5 kW rectifier, a 10 kW electrolyzer, a 28 kg hydrogen tank, and a cycle charging dispatch strategy. The net present cost was $15,360, the

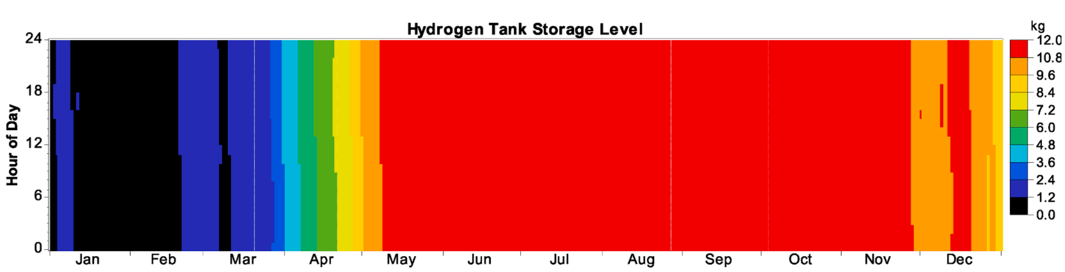

Fig. 7. Monthly hydrogen tank storage level for the optimal energy system of a HADA configuration.

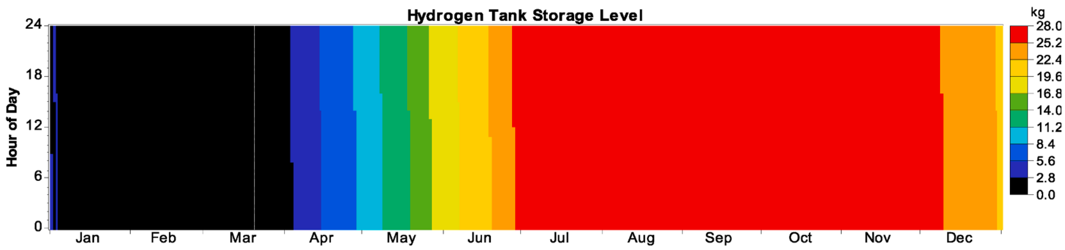

Fig. 8. Monthly hydrogen tank storage level for the optimal energy system of a HAMA configuration.

levelized energy cost was \$0.362/kWh, and the annual running cost was \$403. The PV array represented 44 % of the system's overall cost, while the battery bank represented 42 %. System costs comprised 66 % of the capital costs. The PV system and fuel cell generated a combined electricity production of 6,345 kWh/yr, with the PV system accounting for 95 % and the fuel cell accounting for 5 % of the overall output—the primary load accounted for 3,321 kWh each year, representing 67 % of the total consumption.

Conversely, the electrolyzer consumed ~ 1,672 kWh annually, accounting for 33 % of the overall production. The surplus of renewable energy amounted to 907 kWh/yr. The annual hydrogen output was 36 kg, while the consumption was 19.2 kg. The tank had a storage capacity of over 2,443 h. The net CO_2 emissions were −0.196 kg/yr, indicating a reduction in the CO_2 levels. Additionally, there were 1.11 kg/yr of NOx emissions. The monthly hydrogen tank storage level for the optimal energy system for HAWA configuration indicated the fact that the tank was full between the months of Mid-June and mid-November, while it was at its lowest between the months of January and mid-March (Fig. 9). Similarly, the HAWA battery bank is projected to have a lifetime throughput of 9170 kWh during its expected 10-year lifespan but it is anticipated to achieve a throughput of 455 kWh annually.

Two-Axis tracking

The best system with TA tracking comprised a 5 kW PV array, a 10 kW fuel cell, a 10 kW inverter, a 7.5 kW rectifier, a 10 kW electrolyzer, and a 3 kg hydrogen tank. The TNPC of this system was \$15,113, with a levelized COE of \$0.356 per kWh and an annual running cost of \$614. The PV array represented 44 % of the whole system expenditure, whereas the fuel cell constituted 42 %; the system costs comprised 48 % of the capital costs. The total electricity production was 8,810 kWh/yr, with the PV systems contributing 92 % and fuel cells contributing 8 %. The primary load consumed 3,318 kWh/yr, which accounted for 63 % of the total consumption. The electrolyzer utilized 1,967 kWh each year, which accounted for 37 % of the total energy usage. The surplus of renewable energy amounted to 3,199 kWh/yr. According to Fig. 10, the annual production and consumption of hydrogen were 42 kg, while the tank offered a storage capacity of 262 h. The net CO_2 emissions were −0.432 kg/yr, indicating a reduction in the CO_2 levels. Additionally, there were 2.45 kg/yr of NOx emissions.

Vertical Axis, Continuous Adjustment

The components of the optimal energy system for the VACA tracking, include a 5 kW solar (PV) array, a 3 kW wind turbine, a 10 kW fuel cell, a 10 kW battery bank, an inverter, a rectifier, an electrolyzer, a 28 kg hydrogen tank, and a program that followed the load. With an annual running cost of \$447 and a levelized energy cost of \$0.406 per kWh, the system has a total net present cost of \$17,207. Of the system cost, 39 % was attributable to the PV array and 37 % to the battery bank. Sixty-seven percent of system costs were attributed to capital expenditures. Wind accounted for 5 %, fuel cells for 3 %, and photovoltaics (PV) for 92 % of the total 6,907 kWh/yr. The AC primary load consumed 3,319 kWh/yr (69 %), and 1,507 kWh/yr went to the electrolyzer (or 31 % of consumption). The renewable energy sources produced an excess of 1,659 kWh/yr. The annual output of hydrogen was 32 kg, whereas the yearly consumption was 12.5 kg. The tank had a hydrogen storage autonomy of more than 2,400 h. Renewable energy replacing fossil fuels, resulted in a net CO_2 emissions reduction of −0.128 kg/yr and 0.726 kg/yr of NOx emissions. The system successfully attained a 100 % renewable energy supply by generating more energy than what was needed at a levelized cost of \$0.406/kWh during its projected lifespan. The PV array and battery bank were the primary contributors to the system's overall expenses. Hydrogen production surpassed consumption, allowing for extended storage. The hydrogen level in the tank attached to the optimal energy system indicated that its level peaked between the months of June and December (Fig. 11). The battery connected to the VACA system is projected to have a total energy output of 9170 kWh throughout its anticipated 10-year lifespan; annually, the expected throughput is 384 kWh.

Horizontal Axis, Continuous Adjustment

The optimal system comprised of a 5 kW PV array, a 10 kW fuel cell, a 10 kW inverter, a 7.5 kW rectifier, a 10 kW electrolyzer, and a 12 kg hydrogen tank. The total net present cost was \$15,074, while the levelized energy cost was \$0.355/kWh, and the running cost was \$621 per year. The PV array represented 45 % of the system's overall cost, while the fuel cell accounted for 43 %. The total electricity production was 7,697 kWh per year, with the PV systems accounting for 91 % and the fuel cells contributing 9 %. The primary load consumed 3,319 kWh/yr, which accounted for 59 % of the total consumption. The electrolyzer,

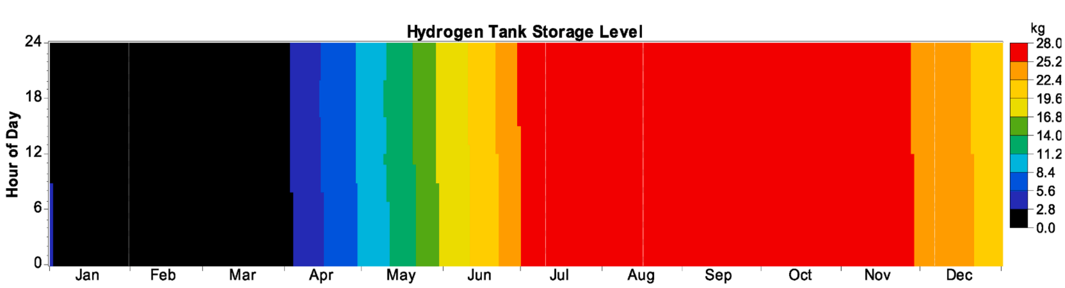

Fig. 9. Monthly hydrogen tank storage level for the optimal energy system of a HAWA configuration.

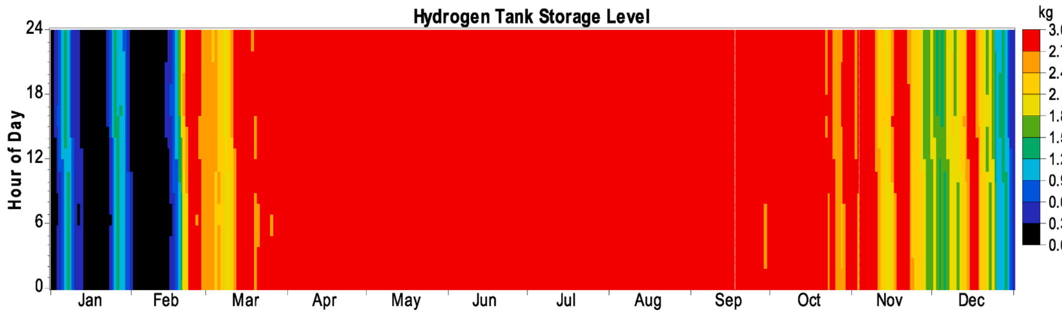

Fig. 10. Monthly hydrogen tank storage level for the optimal energy system of a TA configuration.

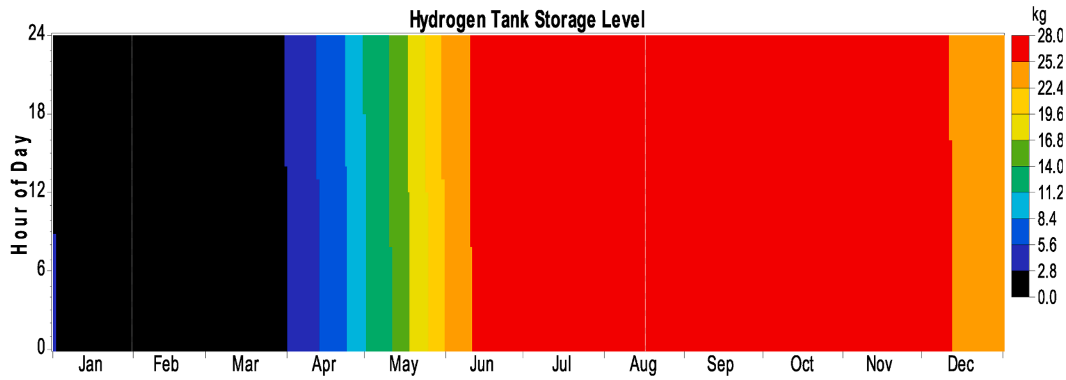

Fig. 11. Monthly hydrogen tank storage level for the optimal energy system of a VACA configuration.

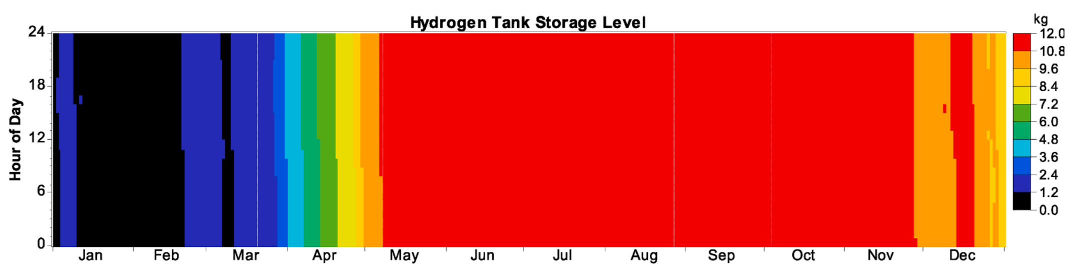

Fig. 12. Monthly hydrogen tank storage level for the optimal energy system of a HACA configuration.

consumed 2,334 kWh annually, accounting for 41 % of the total energy usage. The surplus of renewable energy amounted to 1,719 kWh/yr, while the annual hydrogen output amounted to 50 kg. The yearly consumption amounted to 42.7 kg and the tank offered a storage capacity of 1,047 h. The hydrogen level in the tank, connected to the best energy system, showed a maximum level between the months of June and December and a minimum level between the months of January and February (Fig. 12). The net CO_2 emissions were -0.436 kg/yr, indicating a reduction in CO_2 levels. Additionally, there were 2.48 kg/yr of NOx emissions.

South Africa

The techno-economic results of the viable energy systems for the seven tracking configurations for the South Africa case study is presented in this section

No-Tracking

The optimal system without tracking consisted of a 5 kW photovoltaic array, a 10 kW fuel cell, a 10 kW inverter, a 7.5 kW rectifier, a 10 kW electrolyzer, and a 16 kg hydrogen tank. With a COE of $0.336/kWh, the system had a total net present cost of $14,272 throughout its lifespan, while the operational cost is $626 per year. The fuel cell ($6,530) and PV array ($6,695) were the most significant contributors with regard to net present costs The PV array was responsible for 90 % of the system's total electricity production, or 6,552 kWh annually; it had a 15 % capacity factor and a $0.0799/kWh levelized cost. The fuel cell provides 10 % of the electricity, which had a 50 % mean electrical efficiency and produced 711 kWh annually. This system's monthly hydrogen tank storage level showed that the hydrogen level was at its maximum between the months of June and December (Fig. 13). The energy consumption was entirely sourced from renewable sources, resulting in an annual surplus of 1,136 kWh. However, there was a shortfall of 24.2 kWh in meeting the demand and a capacity shortage of 29.8 kWh. This showed that the system can handle the primary need of 3,323 kWh/year. The fuel cell's annual hydrogen consumption of 42.6 kg was less than the hydrogen production of 53 kg. The hydrogen tank storage allowed 1,396 h of autonomy. Overall, emissions were minimal; nonetheless, 2.47 kg of nitrogen oxides were produced annually.

Horizontal Axis, daily Adjustment

The optimal system architecture under the HADA tracking system,

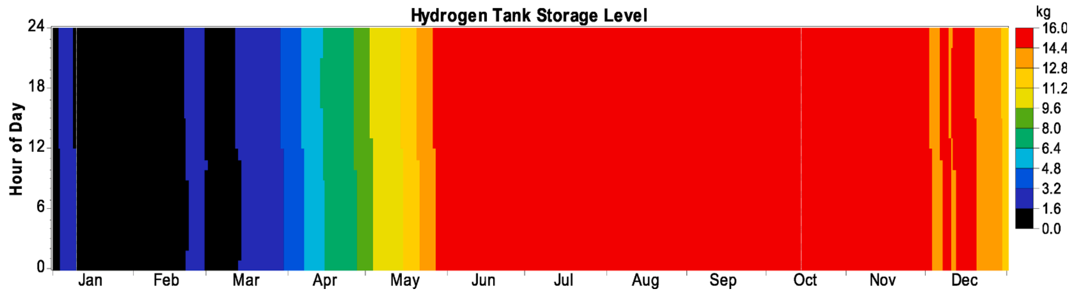

Fig. 13. Monthly hydrogen tank storage level for the optimal energy system of a No tracking configuration.

was a 5 kW photovoltaic array combined with a 10–24 kWh lithium-ion battery bank. The balance of the system, rectifier, and inverter were the other parts. With a levelized COE of $0.339/kWh, the net present cost came to $14,393. With $328 annually, the operating costs were less. The PV array and battery bank were the most significant contributors to capital expenses. The PV array supplied the entire electric load of 8,390 kWh/year. The battery stored the excess PV production, delivering 675 kWh of output per year to the load. The highest average production occurred in the month of October, while the lowest was observed in the month of June (Fig. 14). Most of the months in the year had a power production ranging between 1 to 1.5 kW, except for the period from the months of April to July, during which time, the power production fell below 1 kW.

Horizontal Axis, monthly Adjustment

The HAMA system architecture comprised of a 5 kW PV array, a 10 battery, a 10 kW inverter, and a 7.5 kW rectifier. The cost summary indicated that the TNPC was $14,393, the levelized energy cost was $0.339/kWh, and the yearly running cost was $328. The PV array and the Vision 6FM200D battery substantially contributed to both the initial investment and the expenses for replacing them. The electrical production data showed a surplus of 2,100 kWh/yr, an un-met load of 25.7 kWh/yr, and a renewable portion of 100 %. The photovoltaic (PV) system functioned with a capacity factor of 13.6 %, producing an l energy output of 5,963 kWh/yr. The battery had a nominal capacity of 24.0 kWh and was expected to last 10 years. It had a throughput of 797 kWh/yr. The emissions remained at a constant level of zero, demonstrating the system's exceptional environmental sustainability. Fig. 15 displays the average monthly generation of electricity for the HAMA tracking configuration. The months of December and January experienced the least production. The months of September and October experienced the highest production; the range of the monthly averages was between 0.5 to 0.9 kW. The battery connected to the HAMA configuration has a lifetime throughput of 9,170 kWh and an annual throughput of 791 kWh, indicating continuous and efficient energy delivery over its lifespan.

Horizontal Axis, weekly Adjustment

For the HAWA tracking system, the optimal energy system was a 5 kW solar PV array with 10 Vision 6FM200D batteries that could hold 24 kWh of charge; a 10 kW inverter and a 7.5 kW rectifier were parts of the power circuits. At a levelized cost of $0.339 per kWh, this system design was estimated to have a total net present cost of $14,393 It would also cost $328 per year to run. With an average output of 0.71 kW and a capacity factor of 14.2 %, the PV array generated 6,229 kWh of energy per year. The effective nominal battery capacity was 14.4 kWh, allowing for 37.7 h of self-sufficiency. During a projected lifespan of 10 years, the batteries were estimated to produce a total energy output of 9,170 kW-hours. The system adequately served the energy demand, with an additional annual generation of 2,368 kWh. The solar photovoltaic (PV) penetration was 186 %, indicating that the amount of solar PV energy generated exceed the total energy demand by 86 %. Additionally, the renewable portion was 100 %, meaning that all energy produced was from renewable sources.

Fig. 16. represents a year's average monthly electric production for the HAWA with the lowest production occurring in the months of December and January, while the highest production occurred in the month of October. Production fluctuates throughout the year, growing in the earlier months, peaking in the later months, and then falling at the end of the year. The monthly averages range from 0.52 to 0.96 kW.

Two-Axis tracking

The optimum architecture for the TA system consisted of a 5 kW PV array, a 10 Vision 6FM200D battery, a 10 kW inverter, and a 7.5 kW rectifier. The cost summary revealed a net present cost of $15,030 a levelized cost of energy of $0.354/kWh, and an annual running cost of $328. The electrical production data indicated an excess of 6,611 kWh/yr, an un-met demand of 24.3 kWh/yr, and a renewable energy proportion of 100 %. The PV system ran at a capacity factor of 23.9 %, producing an energy output of 10,470 kWh/yr. The levelized cost of electricity for this system was $0.0500/kWh. The battery had a nominal capacity of 24.0 kWh and it was predicted to have an annual throughput and lifetime throughput of 754 kWh/yr and 9,170 kWh respectively over a lifespan of 10 years.

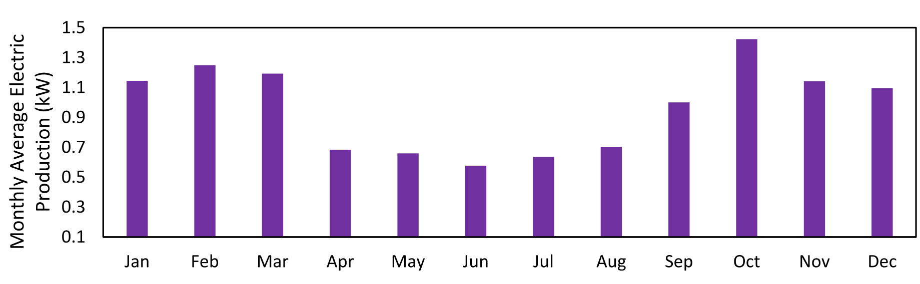

Fig. 14. Monthly Average Electric Production for HADA.

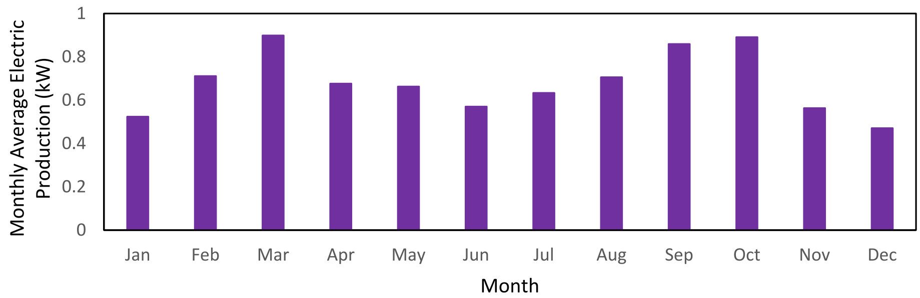

Fig. 15. Monthly Average Electric Production for HAMA.

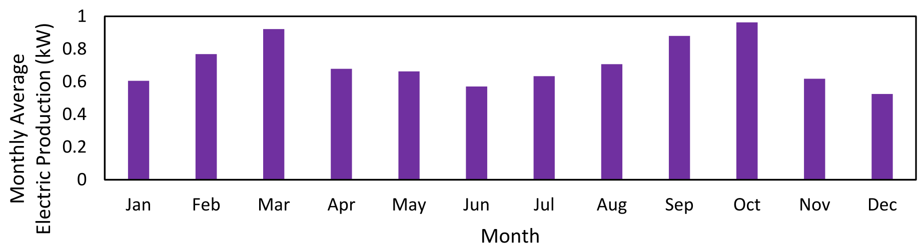

Fig. 16. Monthly Average Electric Production for HAWA.

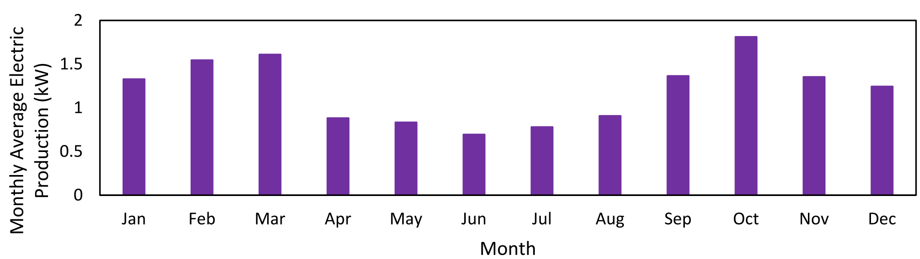

Fig. 17. Monthly Average Electric Production for TA.

Fig. 17 depicts the monthly average electric generation from the TA solar tracking arrangement. Production was lowest in the months of April, May, and June, and highest in the month of October, with monthly averages ranging from 0.69 to 1.81 kW.

Vertical Axis, Continuous Adjustment

The VACA system comprised of a system architecture with a 5 kW photovoltaic (PV) array, a 10 Vision 6FM200D battery, a 10 kW inverter, and a 7.5 kW rectifier. The cost summary revealed a net present cost of $14,285 a levelized cost of energy of $0.336/kWh, and an annual running cost of $328. The PV array and the Vision 6FM200D battery substantially contributed to the capital, replacement, and overall expenses, on an individual component basis. The electrical production data indicated an excess of 2,298 kWh/yr, an un-met demand of 24.0 kWh/yr, and a renewable energy proportion of 100 %. The photovoltaic (PV) system had a capacity factor of 14.1 %, producing an annual energy output of 6,160 kWh/yr with a levelized cost of $0.0850/kWh. The battery had a nominal capacity of 24.0 kWh and an annual throughput of 798 kWh/yr over the period of 10 years. The battery's lifetime throughput is also 9,170 kWh The energy production data for the VACA revealed that the months of December and January experienced the lowest levels of production, whereas September witnessed the highest levels of output (Fig. 18). The monthly averages fluctuated between 0.45 and 0.89 kW.

Horizontal Axis, Continuous Adjustment

The HACA system layout comprised of a 5-kW photovoltaic (PV) array, a 10 Vision 6FM200D battery, a 10 kW inverter, and a 7.5 kW rectifier. The cost study showed that the total net current cost, was $14,900, with a levelized energy cost of $0.351/kWh and an annual

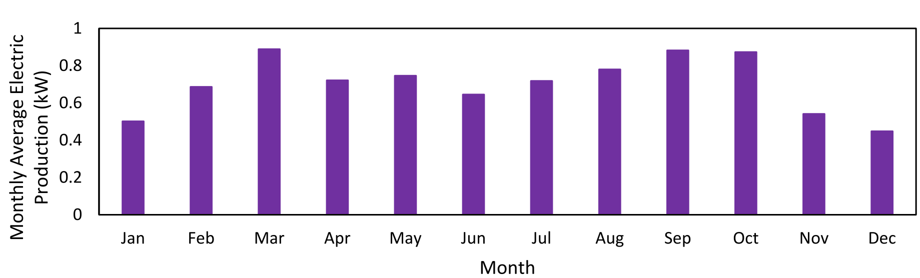

Fig. 18. Monthly Average Electric Production for VACA.

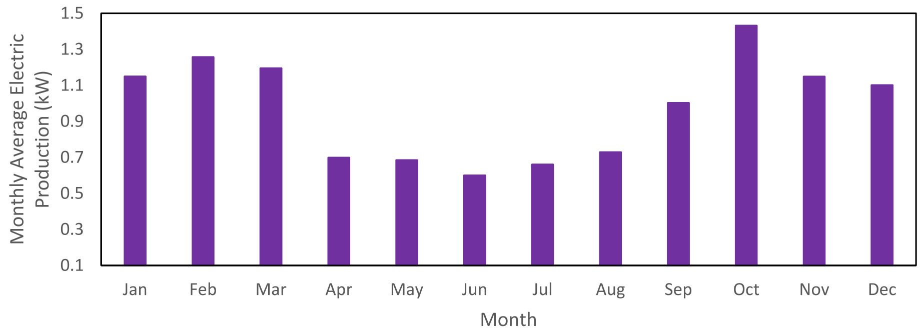

Fig. 19. Monthly Average Electric Production for HACA.

running cost of \$328. The PV array produced 8,507 kWh/yr, resulting in an excess of 4,650 kWh/yr, an unmet demand of 26.2 kWh/yr, and a renewable fraction of 100 %. The photovoltaic (PV) system functioned with a capacity factor of 19.4 %, generating electricity at a levelized cost of \$0.0616/kWh. The 24.0 kWh battery had an average yearly energy output of 753 kWh throughout its 10-year lifespan. For the HACA configuration, the lowest levels of energy production were observed in the months of April, May, and June, while the peak, at 1.432 kW was reached in the month of October with monthly averages ranging from 0.6 to 1.432 kW (Fig. 19).

Water consumption and implications of the electrolyzer

An important aspect of the proposed hybrid renewable energy system is the water consumption of the electrolyzer, which is used to store excess electricity as hydrogen. The electrolyzer in this study has a rated hydrogen production capacity of 10 kW. Based on the annual hydrogen production ranges presented in Table 1 and Table 2, the estimated annual water consumption of the electrolyzer can be calculated using the water consumption rate of 0.9 L/kWh, which is typical for polymer electrolyte membrane (PEM) electrolyzers [22].

For Nigeria, around 48.1 to 53.4 kg/year of hydrogen is produced, which is equal to 1,603 to 1,780 kWh/year (assuming a lower heating value of hydrogen of 33.33 kWh/kg [25]. This means that the electrolyzer in Nigeria would use approximately 1,440 to 1600 L of water per year. Similarly, in South Africa, the annual hydrogen production ranges from 45.3 to 53.3 kg/year (1,510 to 1,776 kWh/year), resulting in an estimated annual water consumption of 1,360 to 1600 L. While these water consumption estimates are low in comparison to the total amount of water used in healthcare institutions, it is critical to evaluate the water source and its consequences for the system's sustainability and resilience. Given the healthcare institutions' rural locations, it is assumed that the electrolyzer will use freshwater obtained from surrounding boreholes or wells. If the water quality does not satisfy the electrolysis specifications, a simple filtration and purification device can be used to pre-treat the water [19].

However, in areas with limited freshwater resources, using seawater for electrolysis could be considered as another option. This would involve making important changes to the design of the electrolyzer, like using materials that can resist corrosion and implementing more advanced filtration and pretreatment systems. These modifications are likely to make the electrolyzer subsystem more expensive to build and maintain [30]. In the future, researchers could conduct studies to assess whether it's practical and financially viable to use seawater for electrolysis in hybrid renewable energy systems for rural healthcare facilities. The water requirement for the electrolyzer may have a long-term implication regarding sustainability and resilience in the development of the proposed hybrid renewable system. On the other hand, the possible use of seawater has a corresponding potential in future works to optimize system design and economics, especially in areas that are water scarce.

Multi-criterial-decision-making results

This section presents the results of the MCDM analysis by using EDAS; as opposed to using the ideal or optimal answer; EDAS uses the average solution as a benchmark. As a result, it is less susceptible to extremes in the criteria values. The results of the EDAS method were validated by using the TOPSIS method; this was selected because of its ability to establish positive and negative ideal reference points, offering a valuable benchmark for comparison.

The first step in implementing EDAS is to determine the initial decision matrix. This matrix usually entails the determination of the alternatives (in this case the best energy systems for each tracking system) and the criteria (obtained from the energy simulation results). This study selects the Total NPC, COE, LCOH, Capacity Shortage, Total Electrical Production, and Excess Electricity as criteria. These criteria cover factors that are related to economic and technical constraints. The alternative includes optimal systems for: NT, HADA, HAMA, HAWA, TA, VACA and HACA tracking configurations. Hence, the initial decision matric is given, as shown in Eq. (14).

$$X = [X_{ij}]_{q\times p} = \begin{bmatrix} x_{11} & x_{12} & \cdots & x_{1p} \\ x_{21} & x_{22} & \cdots & x_{2p} \\ \vdots & \vdots & \vdots & \vdots \\ x_{q1} & x_{q2} & \cdots & x_{qp} \end{bmatrix} \tag{14}$$

$0 \leq x_{ij}$

$i \in \{1, 2, \ldots q\}$ and $j \in \{1, 2, \ldots p\}$.

The elements of the matrix are obtained from Tables 1 and 2 (optimization the results from Nigeria and South Africa). The initial decision matrix for the Nigeria case study, is given in Eq. (14).

$$X_{ij} = \begin{bmatrix} 14272 & 0.336 & 20.9 & 30 & 7263 & 1136 \\ 14612 & 0.344 & 22.6 & 33 & 7556 & 1567 \\ 16103 & 0.38 & 38.5 & 37 & 6255 & 1000 \\ 15360 & 0.362 & 33.3 & 33 & 6345 & 907 \\ 15113 & 0.356 & 27.9 & 36 & 8810 & 3199 \\ 17207 & 0.406 & 41.5 & 35 & 6907 & 1659 \\ 16229 & 0.382 & 24.4 & 33 & 7206 & 3394 \end{bmatrix} \tag{15}$$

The next step is to obtain the average solution AV_j, a 1×6 matrix, obtained by dividing the sum of the elements x_{ij} for each criterion, by the number of elements n, as given in Eq. (15). When this is implemented, it results in Eq. (16).

$$AV_j = \frac{\sum_{i=1}^{n} x_{ij}}{n} \tag{16}$$

when Eq. (15) is implemented, it results in Eq. (17).

$$AV_j = [15,557 \quad 0.3666 \quad 30 \quad 34 \quad 7,192 \quad 1,837] \tag{17}$$

The next step in implementing the EDAS, is the estimation of the positive distance from the average $[PDA_{ij}]_{q\times p}$ and the corresponding negative distance from the average $[NDA_{ij}]_{q\times p}$ by using Eqs. (17) and (18), respectively; these yielded the matrices in Eqs. (19) and (20).

$$\mathrm{PDA}_{ij} = \begin{cases} \dfrac{max(0,(X_{ij} - AV_j))}{AV_j}, ifj^{th} criterionisbeneficial \\ \dfrac{max(0,(AV_j - X_{ij}))}{AV_j}, ifj^{th} criterionisnon-beneficial \end{cases} \tag{18}$$

$$\mathrm{NDA}_{ij} = \begin{cases} \dfrac{max(0,\ (\mathrm{AV_j} - \mathrm{X_{ij}}))}{\mathrm{AV_j}}, ifj^{th} criterionisbeneficial \\ \dfrac{max(0,\ (\mathrm{X_{ij}} - \mathrm{AV_j}))}{\mathrm{AV_j}}, ifj^{th} criterionisnon-beneficial \end{cases} \tag{19}$$

$$\mathrm{PDA}_{ij} = \begin{bmatrix} 0.0826 & 0.0834 & 0.3003 & 0.1139 & 0.0099 & 0.0000 \\ 0.0607 & 0.0616 & 0.2434 & 0.0253 & 0.0507 & 0.0000 \\ 0.0000 & 0.0000 & 0.0000 & 0.0000 & 0.0000 & 0.0000 \\ 0.0126 & 0.0125 & 0.0000 & 0.0253 & 0.0000 & 0.0000 \\ 0.0285 & 0.0288 & 0.0660 & 0.0000 & 0.2250 & 0.7410 \\ 0.0000 & 0.0000 & 0.0000 & 0.0000 & 0.0000 & 0.0000 \\ 0.0000 & 0.0000 & 0.1832 & 0.0253 & 0.0020 & 0.8471 \end{bmatrix} \tag{20}$$

$$\mathrm{NDA}_{ij} = \begin{bmatrix} 0.0000 & 0.0000 & 0.0000 & 0.0000 & 0.0099 & 0.0000 \\ 0.0000 & 0.0000 & 0.0000 & 0.0000 & 0.0507 & 0.0000 \\ 0.0351 & 0.0366 & 0.2889 & 0.0928 & 0.0000 & 0.0000 \\ 0.0000 & 0.0000 & 0.1148 & 0.0000 & 0.0000 & 0.0000 \\ 0.0000 & 0.0000 & 0.0000 & 0.0633 & 0.2250 & 0.7410 \\ 0.1061 & 0.1076 & 0.3893 & 0.0338 & 0.0000 & 0.0000 \\ 0.0432 & 0.0421 & 0.0000 & 0.0000 & 0.0020 & 0.8471 \end{bmatrix} \tag{21}$$

Following the estimation of the positive and negative distances from the average, the alternatives' weighted sums of PDA and NDA (SP_i and SN_i), are calculated by multiplying $[PDA_{ij}]_{q\times p}$ and $[NDA_{ij}]_{q\times p}$ with the weight of the criteria, denoted as w_j by using Eqs. (22) and (23), respectively. The weight, w_j is usually greater than 0 and does not exceed 1; in addition, the sum of the weights of the criteria must be equal to 1. The CRITIC method is used to calculate the criteria weights and for the CRITIC method, the weights obtained are from Eq. (23). For the Nigerian case study, excess electricity had the highest weight of 28.87 %, while the criterion with the least weight was the levelized cost of hydrogen (Fig. 20). With regards to the South African case, the Total Electricity Production, and the Total NPC, had the highest and lowest contributions of 22.22 % and 12.74 %, respectively (Fig. 20).

$$SP_i = \sum_{j=1}^{m} w_j PDA_{ij} \tag{22}$$

$$SN_i = \sum_{j=1}^{m} w_j NDA_{ij} \tag{23}$$

where:

$$w_j = \begin{bmatrix} 0.1314 \\ 0.1298 \\ 0.1153 \\ 0.1745 \\ 0.1603 \\ 0.2887 \end{bmatrix} \tag{24}$$

The product of the weights (w_j) and the PDA_{ij} and NDA_{ij} for the Nigerian case, is obtained thus:

$$WPDA_{ij} = \begin{bmatrix} 0.0108 & 0.0108 & 0.0346 & 0.0199 & 0.0016 & 0.0000 \\ 0.0080 & 0.0080 & 0.0281 & 0.0044 & 0.0081 & 0.0000 \\ 0.0000 & 0.0000 & 0.0000 & 0.0000 & 0.0000 & 0.0000 \\ 0.0017 & 0.0016 & 0.0000 & 0.0044 & 0.0000 & 0.0000 \\ 0.0037 & 0.0037 & 0.0076 & 0.0000 & 0.0361 & 0.2140 \\ 0.0000 & 0.0000 & 0.0000 & 0.0000 & 0.0000 & 0.0000 \\ 0.0000 & 0.0000 & 0.0211 & 0.0044 & 0.0003 & 0.2446 \end{bmatrix} \tag{25}$$

$$WNDA_{ij} = \begin{bmatrix} 0.0000 & 0.0000 & 0.0000 & 0.0000 & 0.0016 & 0.0000 \\ 0.0000 & 0.0000 & 0.0000 & 0.0000 & 0.0081 & 0.0000 \\ 0.0046 & 0.0048 & 0.0333 & 0.0162 & 0.0000 & 0.0000 \\ 0.0000 & 0.0000 & 0.0132 & 0.0000 & 0.0000 & 0.0000 \\ 0.0000 & 0.0000 & 0.0000 & 0.0110 & 0.0361 & 0.2140 \\ 0.0139 & 0.0140 & 0.0449 & 0.0059 & 0.0000 & 0.0000 \\ 0.0057 & 0.0055 & 0.0000 & 0.0000 & 0.0003 & 0.2446 \end{bmatrix} \tag{26}$$

$$SP_i = \begin{bmatrix} 0.0778 \\ 0.0566 \\ 0.0000 \\ 0.0077 \\ 0.2651 \\ 0.0000 \\ 0.2705 \end{bmatrix} \tag{27}$$

$$SN_i = \begin{bmatrix} 0.0778 \\ 0.0566 \\ 0.0000 \\ 0.0077 \\ 0.2651 \\ 0.0000 \\ 0.2705 \end{bmatrix} \tag{28}$$

The next step is to normalize the weighted sum of the PDA and NDA by employing Eqs. (29) and (30) to obtain the following matrices:

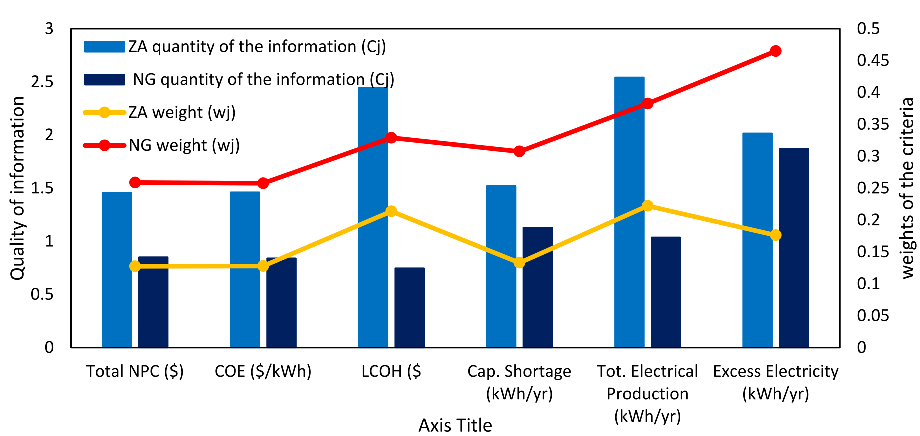

Fig. 20. Quality of information and weights of the criteria by using the CRITIC method.

$$NSP_i = \frac{SP_i}{max_i(SP_i)} = \begin{bmatrix} 0.2875 \\ 0.2092 \\ 0.0000 \\ 0.0285 \\ 0.9803 \\ 0.0000 \\ 1.0000 \end{bmatrix} \tag{29}$$

$$NSN_i = \frac{SN_i}{max_i(SN_i)} = \begin{bmatrix} 0.9939 \\ 0.9689 \\ 0.7745 \\ 0.9493 \\ 0.0000 \\ 0.6987 \\ 0.0192 \end{bmatrix} \tag{30}$$

The assessment score for each energy system alternative is obtained by using Eq. (31). The values of the assessment score were used to rank the alternatives. The results of the EDAS assessment for the South African case study is presented in Table 3; these include the values for SP_i, SN_i. NSP_i, NSN_i, and AS_i. By using the assessment scores for both case studies, the most preferred energy technology for the Nigerian case study, is the one that used the non-tracking device, while the least preferred, is the energy system with a VACA technology (Fig. 21). For the South African case, the energy system HAMA tracking technology was the most preferred, while the energy system without a tracking system is the most preferred (Fig. 21).

$$AS_i = \frac{(NSP_i + NSN_i)}{2} = \begin{bmatrix} 0.6407 \\ 0.5890 \\ 0.3872 \\ 0.4888 \\ 0.4901 \\ 0.3493 \\ 0.50959 \end{bmatrix} \tag{31}$$

Table 4 compares the results of this present and similar studies. Dekkiche et al., [20] reveal that Vertical Single-Axis Trackers are the most economically feasible, contrasting with [24]'s emphasis on improved energy harvest and reduced NPC with horizontal and dual trackers. Hosseini Dehshiri et al. highlighted the significant electricity generation increase with Two-Axis (TA) systems, contrasting with [12]'s regional optimization focus, which identified daily adjusted horizontal axis trackers as the best for Nigeria. However, Hosseini Dehshiri & Firoozabadi, [24]'s result aligns with that obtained by Babatunde et al. which identified Dual Axis as optimal for the South African case. This present study shows that based on the techno-economic results, the optimal energy system for the Nigerian case is the energy arrangement without tracking devices, while the best system for the South African healthcare facility is the one with HAWA tracking. The findings emphasize the complex nature of HRES design, which is influenced by economic, technological, and regional factors. Efficient system design necessitates the harmonization of economic viability and energy production capacity, employing appropriate monitoring configurations tailored to specific project objectives and geographical circumstances.

By and large, this study's findings present some novel results. First, the techno-economic analysis shows that the proposed hybrid renewable energy systems for rural healthcare institutions in Nigeria and South Africa are feasible and cost-effective. This agrees with the study carried out by Babatunde et al. for another application in both South Africa and Nigeria [11]. The optimal energy designs can supply electricity demands at competitive costs, with LCOEs ranging from \$0.340–0.410/kWh in Nigeria and \$0.336–0.354/kWh in South Africa. Furthermore, the analysis of various solar tracking arrangements reveals their impact on energy production, costs, and overall system viability, introducing a new viewpoint to evaluating hybrid systems for rural healthcare centers. The findings of this study have broader implications that extend beyond the specific case studies of rural healthcare facilities in Nigeria and South Africa. The methods and insights acquired can be utilized in other locations facing similar energy access and healthcare delivery challenges. The comprehensive techno-economic analysis, integration of various solar tracking configurations, and utilization of the EDAS approach for MCDM analysis provide a framework for assessing the viability and enhancing the design of hybrid renewable energy systems in other regions. The system designs, which integrate solar PV, wind turbines, batteries, and hydrogen storage, can be adapted to suit different locations' specific conditions and requirements.

Table 3
EDAS assessment results for the South African case study.

Tracking Configuration	Spi	Sni	Nspi	Nsni	Asi
NT	0.1233	0.6945	0.6605	0.0000	0.3303
HADA	0.1475	0.0891	0.7903	0.8718	0.8310
HAMA	0.1866	0.0028	1.0000	0.9960	0.9980
HAWA	0.1728	0.0028	0.9260	0.9960	0.9610
TA	0.1767	0.2369	0.9469	0.6590	0.8029
VACA	0.1758	0.0000	0.9418	1.0000	0.9709
HACA	0.1476	0.1044	0.7911	0.8497	0.8204

Conclusion

Access to reliable and sustainable power in developing countries' rural areas remains a major issue. This study examined the technical and economic performances of solar PV/wind/battery/fuel cell hybrid systems for off-grid primary healthcare clinics in Sub-Saharan Africa. The HOMER software was used to design and simulate optimal hybrid renewable energy systems for Nigeria and South Africa, as case studies. This study provides novel insights into the subject of hybrid renewable energy systems for rural healthcare facilities in sub-Saharan Africa. The comprehensive techno-economic analysis, assessment of solar tracking configurations, and utilization of the EDAS approach for MCDM analysis offer innovative perspectives on these systems' viability, optimization, and decision-making procedures. The results emphasize the potential impact of hybrid renewable energy systems on bridging the gap between energy access and healthcare delivery in rural areas, while also supporting the global initiatives to accomplish Sustainable Development Goals 3 and 7 and reduce the effects of climate change.

The findings demonstrate the practicality of supplying energy to rural clinics by using solar photovoltaic (PV) systems, wind power, batteries, and hydrogen storage. The hybrid systems developed, can efficiently meet the electrical demands of health the facilities in Nigeria and South Africa, with levelized energy costs ranging from \$0.340–0.410/kWh and \$0.336–0.354/kWh, respectively. The proposed hybrid systems can provide reliable power, facilitating healthcare service delivery and enhancing quality of life. This aligns with the Sustainable Development Goals (SDGs) 3 and 7.

The hybrid systems leverage abundant local solar and wind resources, aligning with SDG 7′s call for sustainable energy access. Nigeria's annual power production ranges from 6,255 to 8,810 kWh, while South Africa's ranges from 5,963 to 10,470 kWh. Solar photovoltaic (PV) technology accounts for over 90 % of this energy production. The research provides an effective framework for context-specific planning and adopting renewable hybrids for off-grid health facilities. Although greater proportions of renewable energy sources lead to a decrease in the cost of electricity (COE) and emissions, they also significantly increase the initial investment required. To make hybrid systems more affordable, governments should institute policies that can be of help, such as: subsidies, incentives, and financing schemes to the operators of the hybrid systems. Positive signs for increasing electrification in the rural areas include a declining COE trend due to an increase in the incorporation of renewable energy sources. A decrease in COE enhances the availability of power and drives socioeconomic development in outlying regions.

The proposed hybrid energy system can mitigate the associated environmental concerns by replacing diesel generators. The emissions

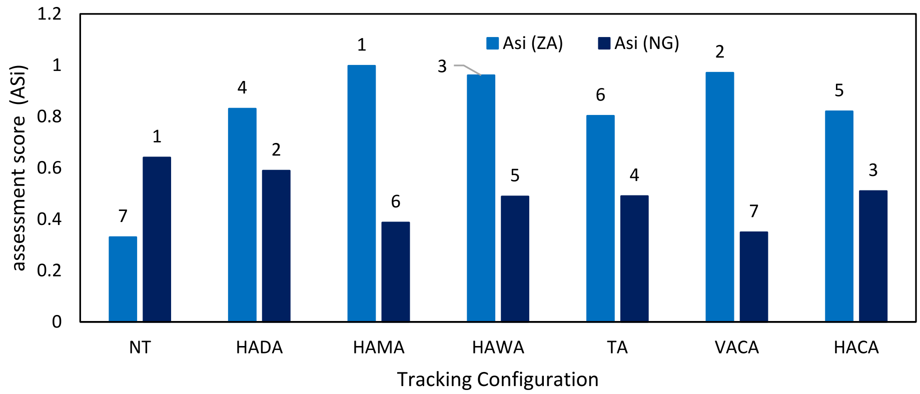

Fig. 21. Ranking of the energy systems.

Table 4
Comparison of the present study with relevant studies.

Study	Location	Hybrid System	Solar Tracking Configurations	Key Findings
[20]	Algeria	PV/ Reformer/FC	4 configurations	Vertical Single Axis Tracker (VSAT) had the best economic performance with low NPC and COE.
[24]	Iran	PV (grid-connected)	4 configurations	Two-Axis (TA) system generated 31.8 % more electricity than Fixed Tilt (FT). Horizontal tracking systems had 8.8 % higher LCOE than FT.
[11]	South Africa and Nigeria	PV/Wind/ FC/Battery	7 configurations	Nigeria: Optimal system with TNPC of $9421 and COE of $0.754/kWh. South Africa: Optimal system with TNPC of $8771 and COE of $0.701/kWh.
[5]	Sudan and South Sudan	PV/DG/ESS	2 configurations	Horizontal and dual solar trackers provided up to 50 % better energy harvest and reduced NPC by up to 7 %. Solar tracking feasible if costs < 375 USD (Sudan) and 250 USD (South Sudan).
Present study	Nigeria and South Africa	PV/Wind/ Battery/Fuel Cell/ Hydrogen Storage	7 configurations	Nigeria: LCOE $0.336–0.410/ kWh, Optimal system (NT) with TNPC $14,272 and COE $0.336/kWh. South Africa: LCOE $0.336–0.354/ kWh, Optimal system (HAMA) with TNPC $14,393 and COE $0.339/ kWh

decrease by between 90–100 %, with yearly NOx emissions ranging between 0.726–2.48 kg in Nigeria and 0 kg in South Africa. The NOx emission results from the air intake of contaminants, anode reactions, catalyst activity, operating conditions, and fuel impurities. The study demonstrates the feasibility of solar PV/wind/battery systems in delivering sustainable and reliable energy access to enhance healthcare, therefore, promoting the achievement of Sustainable Development Goals 3 and 7.

This research has proven that it is feasible to power healthcare facilities in Sub-Saharan Africa with sustainable and efficiently designed hybrid renewable systems. By employing efficient system design, PV/ wind/battery hybrids offer a practical alternative for extending power supply to facilitate healthcare service delivery, therefore, effectively addressing the issue of intermittent electricity supplies in the primary health sectors in Sub-Saharan Africa. The study provides a significant framework that can adequately assist in the planning of tailored to the specific circumstances of un-electrified rural communities in the region, with the desire to attain the aims of the Sustainable Development Goals 3 and 7.

CRediT authorship contribution statement

Oluwaseye Samson Adedoja: Writing – original draft, Visualization, Validation, Software, Methodology, Investigation, Formal analysis, Data curation, Conceptualization. **Emmanuel Rotimi Sadiku:** Writing – review & editing, Visualization, Validation, Supervision. **Yskandar Hamam:** Writing – review & editing, Visualization, Validation, Supervision.

Declaration of competing interest

The authors declare that they have no known competing financial interests or personal relationships that could have appeared to influence the work reported in this paper.

Data availability

Data will be made available on request.

Acknowledgments

The authors thank the Tshwane University of Technology, Pretoria, South Africa, for their support and for providing an enabling environment.

Appendix A. Supplementary data

Supplementary data to this article can be found online at https://doi.org/10.1016/j.ecmx.2024.100643.

References

[1] Abdulsalam KA, Adebisi J, Emezirinwune M, Babatunde O. An overview and multicriteria analysis of communication technologies for smart grid applications. E-Prime-Adv Electrical Eng, Electronics and Energy 2023;3:100121.
[2] Adedoja OS. Hybrid power system for a fuel station considering temperature coefficient. Int J Energy Econ Policy 2020.
[3] Adedoja OS, Saleh UA, Alesinloye AR, Timiyo T-E-J, Onuigbo IF, Adejuwon OO, et al. An energy balance and multicriterial approach for the sizing of a hybrid renewable energy system with hydrogen storage. E-Prime-Adv Electrical Eng, Electronics and Energy 2023;4:100146.
[4] Adetoro SA, Olatomiwa L, Tsado J, Dauda SM. Techno-economic and environmental impact assessment of a hybrid renewable energy system employing an enhanced combined dispatch strategy. Green Energy and Resources 2023;1(4): 100044.
[5] Ahmed EEE, Demirci A, Tercan SM. Optimal sizing and techno-enviro-economic feasibility assessment of solar tracker-based hybrid energy systems for rural electrification in Sudan. Renew Energy 2023;205:1057–70. https://doi.org/10.1016/J.RENENE.2023.02.022.
[6] Alsagri AS, Alrobaian AA, Nejlaoui M. Techno-economic evaluation of an off-grid health clinic considering the current and future energy challenges: a rural case study. Renew Energy 2021;169:34–52.
[7] Alshammari N, Samy MM, Asumadu J. Optimal economic analysis study for renewable energy systems to electrify remote region in Kingdom of Saudi Arabia. Twentieth Int Middle East Power Systems Conference (MEPCON) 2018;2018: 1040–5.
[8] Ayodele TR, Mosetlhe TC, Yusuff AA, Ogunjuyigbe ASO. Off-grid hybrid renewable energy system with hydrogen storage for South African rural community health clinic. Int J Hydrogen Energy 2021.
[9] Babatunde O, Denwigwe I, Oyebode O, Ighravwe D, Ohiaeri A, Babatunde D. Assessing the use of hybrid renewable energy system with battery storage for power generation in a University in Nigeria. Environ Sci Pollut Res 2022;29(3): 4291–310.
[10] Babatunde OM, Munda JL, Hamam Y. A comprehensive state-of-the-art survey on hybrid renewable energy system operations and planning. IEEE Access 2020.
[11] Babatunde OM, Munda JL, Hamam Y. Hybridized off-grid fuel cell/wind/solar PV/ battery for energy generation in a small household: a multi-criteria perspective. Int J Hydrogen Energy 2022;47(10):6437–52.
[12] Babatunde OM, Munda JL, Hamam Y. Off-grid hybrid photovoltaic–micro wind turbine renewable energy system with hydrogen and battery storage: effects of sun tracking technologies. Energ Conver Manage 2022;255:115335.
[13] Babatunde OM, Oluseyi PO, Akinbulire TO, Denwigwe HI, Akin-Adeniyi TJ. The role of demand-side management in carbon footprint reduction in modern energy services for rural health clinics. In: Environmental Carbon Footprints. Elsevier; 2018. p. 317–63.
[14] Babatunde OM, Adedoja OS, Babatunde DE, D. IH. (2019). Off- grid hybrid renewable energy system for rural healthcare centers: A case study in Nigeria. *Energy Science & Engineering*, *00*, 1–18. https://doi.org/OS, Babatunde DE, Denwigwe IH. Off- grid hybrid renewable energy system for rural healthcare centers: A case study in Nig. doi.org/10.1002/ese3.314.
[15] Babayomi OO, Olubayo B, Denwigwe IH, Somefun TE, Adedoja OS, Somefun CT, et al. A review of renewable off-grid mini-grids in Sub-Saharan Africa. Front Energy Res 2023;10:1089025. https://doi.org/10.3389/FENRG.2022.1089025/BIBTEX.
[16] Barakat S, Emam A, Samy MM. Investigating grid-connected green power systems' energy storage solutions in the event of frequent blackouts. Energy Rep 2022;8: 5177–91.
[17] Chakamera C, Alagidede P. Electricity crisis and the effect of CO2 emissions on infrastructure-growth nexus in Sub Saharan Africa. Renew Sustain Energy Rev 2018;94:945–58.
[18] Chowdhury T, Chowdhury H, Hasan S, Rahman MS, Bhuiya MMK, Chowdhury P. Design of a stand-alone energy hybrid system for a makeshift health care center: a case study. J Building Eng 2021;40:102346.
[19] Dedigama I, Angeli P, Van Dijk N, Millichamp J, Tsaoulidis D, Shearing PR, et al. Current density mapping and optical flow visualisation of a polymer electrolyte membrane water electrolyser. J Power Sources 2014;265:97–103. https://doi.org/10.1016/J.JPOWSOUR.2014.04.120.
[20] Dekkiche M, Tahri T, Denai M. Techno-economic comparative study of grid-connected PV/reformer/FC hybrid systems with distinct solar tracking systems. Energy Conversion and Management: X 2023;18:100360. https://doi.org/10.1016/J.ECMX.2023.100360.
[21] Elkadeem MR, Wang S, Sharshir SW, Atia EG. Feasibility analysis and techno-economic design of grid-isolated hybrid renewable energy system for electrification of agriculture and irrigation area: a case study in Dongola, Sudan. Energ Conver Manage 2019;196:1453–78.
[22] El-Shafie M. Hydrogen production by water electrolysis technologies: a review. Results in Eng 2023;20:101426. https://doi.org/10.1016/J.RINENG.2023.101426.
[23] Ghorabaee MK, Zavadskas EK, Amiri M, Turskis Z. Extended EDAS method for fuzzy multi-criteria decision-making: an application to supplier selection. Int J Computers, Communications and Control 2016. https://doi.org/10.15837/ijccc.2016.3.2557.
[24] Hosseini Dehshiri SS, Firoozabadi B. Comparison, evaluation and prioritization of solar photovoltaic tracking systems using multi criteria decision making methods. Sustainable Energy Technol Assess 2023;55:102989. https://doi.org/10.1016/J.SETA.2022.102989.
[25] Ibrahim OS, Singlitico A, Proskovics R, McDonagh S, Desmond C, Murphy JD. Dedicated large-scale floating offshore wind to hydrogen: assessing design variables in proposed typologies. Renew Sustain Energy Rev 2022;160:112310. https://doi.org/10.1016/J.RSER.2022.112310.
[26] IEA International Energy Agency. (2020). *Covid-19 reverses electricity access progress*. https://www.iea.org/reports/sdg7-data-and-projections/access-to-electricity.
[27] Ighravwe D, Babatunde M. Selection of a mini-grid business model for developing countries using CRITIC-TOPSIS with interval type-2 fuzzy sets. Decision Sci Lett 2018;7(4):427–42.
[28] Ighravwe DE, OM B, Adedoja OS, Okharedia TE. Evaluation and selection of hybrid renewable energy systems for healthcare centres in rural areas: a techno-economic approach. 2018 IEEE 7th Int Conference on Adaptive Sci & Technol (ICAST) 2018: 1–7.
[29] Islam MMM, Kowsar A, Haque AKMM, Hossain MK, Ali MH, Rubel MHK, et al. Techno-economic analysis of hybrid renewable energy system for healthcare centre in northwest Bangladesh. Process Integration and Optimization for Sustainability 2023;7(1–2):315–28.
[30] Khan MA, Al-Attas T, Roy S, Rahman MM, Ghaffour N, Thangadurai V, et al. Seawater electrolysis for hydrogen production: a solution looking for a problem? Energ Environ Sci 2021;14(9):4831–9. https://doi.org/10.1039/D1EE00870F.
[31] Koholé YW, Fohagui FCV, Djiela RHT, Tchuen G. Wind energy potential assessment for co-generation of electricity and hydrogen in the far North region of Cameroon. Energ Conver Manage 2023;279:116765. https://doi.org/10.1016/J.ENCONMAN.2023.116765.
[32] Koholé YW, Fohagui FCV, Ngouleu CAW, Tchuen G. An effective sizing and sensitivity analysis of a hybrid renewable energy system for household, multi-media and rural healthcare centres power supply: a case study of Kaele, Cameroon. Int J Hydrogen Energy 2024;49:1321–59.
[33] Koholé YW, Ngouleu CAW, Fohagui FCV, Tchuen G. Quantitative techno-economic comparison of a photovoltaic/wind hybrid power system with different energy storage technologies for electrification of three remote areas in Cameroon using Cuckoo search algorithm. J Storage Mater 2023;68:107783.
[34] Ngouleu CAW, Koholé YW, Fohagui FCV, Tchuen G. Optimal sizing and techno-enviro-economic evaluation of a hybrid photovoltaic/wind/diesel system with battery and fuel cell storage devices under different climatic conditions in Cameroon. J Clean Prod 2023;423:138753.
[35] Ngouleu CAW, Koholé YW, Fohagui FCV, Tchuen G. Techno-economic analysis and optimal sizing of a battery-based and hydrogen-based standalone photovoltaic/wind hybrid system for rural electrification in Cameroon based on meta-heuristic techniques. Energ Conver Manage 2023;280:116794.
[36] Ohunakin OS, Adaramola MS, Oyewola OM, Fagbenle RO, Adelekan DS, Gill J, et al. Photovoltaic performance prediction in Northern Nigeria using generated typical meteorological year dataset. Afr J Sci Technol Innov Dev 2018;10(5): 579–91.
[37] Olatomiwa L, Longe OM, Abd'Azeez TA, Ambafi JG, Jack KE, Sadiq AA. Optimal planning and deployment of hybrid renewable energy to rural healthcare facilities in Nigeria. Energies 2023;16(21):7259.
[38] Olatomiwa L, Mekhilef S, Ohunakin OS. Hybrid renewable power supply for rural health clinics (RHC) in six geo-political zones of Nigeria. Sustainable Energy Technol Assess 2016;13:1–12.
[39] Ouedraogo NS, Schimanski C. Energy poverty in healthcare facilities: a "silent barrier" to improved healthcare in sub-Saharan Africa. J Public Health Policy 2018;39:358–71.
[40] Purewal J, Wang J, Graetz J, Soukiazian S, Tataria H, Verbrugge MW. Degradation of lithium ion batteries employing graphite negatives and nickel–cobalt–manganese oxide + spinel manganese oxide positives: Part 2, chemical–mechanical degradation model. J Power Sources 2014;272:1154–61. https://doi.org/10.1016/J.JPOWSOUR.2014.07.028.
[41] Raghuwanshi SS, Arya R. Design and economic analysis of a stand-alone hybrid photovoltaic energy system for remote healthcare centre. Int J Sustain Eng 2020;13 (5):360–72.
[42] Raghuwanshi SS, Arya R. Reliability evaluation of stand-alone hybrid photovoltaic energy system for rural healthcare centre. Sustainable Energy Technol Assess 2020; 37:100624.
[43] Samy, M. M., Barakat, S. (2019). Hybrid invasive weed optimization-particle swarm optimization algorithm for biomass/PV micro-grid power system. *2019 21st International Middle East Power Systems Conference (MEPCON)*, 377–382.
[44] Samy MM, Emam A, Tag-Eldin E, Barakat S. Exploring energy storage methods for grid-connected clean power plants in case of repetitive outages. J Storage Mater 2022;54:105307.
[45] Sodiq A, Baloch AAB, Khan SA, Sezer N, Mahmoud S, Jama M, et al. Towards modern sustainable cities: review of sustainability principles and trends. J Clean Prod 2019;227:972–1001.
[46] Tazay AF, Samy MM, Barakat S. A techno-economic feasibility analysis of an autonomous hybrid renewable energy sources for university building at Saudi Arabia. J Electr Eng Technol 2020;15:2519–27.
[47] World Bank. (2021). *Report: Universal Access to Sustainable Energy Will Remain Elusive Without Addressing Inequalities*. https://www.worldbank.org/en/news/press-release/2021/06/07/report-universal-access-to-sustainable-energy-will-remain-elusive-without-addressing-inequalities#:~:text=Globally%2C the number of people,to 759 million in 2019.
[48] Yakub AO, Same NN, Owolabi AB, Nsafon BEK, Suh D, Huh J-S. Optimizing the performance of hybrid renewable energy systems to accelerate a sustainable energy transition in Nigeria: a case study of a rural healthcare centre in Kano. Energ Strat Rev 2022;43:100906.